

Claude E. Duchon*

School of Meteorology, University of Oklahoma, Norman, OK

Charles G. Wade and Jeffery A. Cole

Research Applications Program, National Center for Atmospheric Research, Boulder, CO

1. INTRODUCTION

Beginning spring 2000 an investigation was initiated to compare observed responses of vibrating wires in Geonor precipitation gauges using factory-provided coefficients in the calibration equation with expected responses calculated using known weights. A comparison of this kind is called a calibration-verification, that is, the goal is to verify the calibration. Two Geonor gauges were supplied by USCRN (United States Climate Reference Network), each with three vibrating wires along with a Campbell Scientific, Inc. CR10 data logger. The two gauges were placed in a Thermotron temperature-controlled 1-m³ chamber when calibration-verifications were performed at temperatures below room temperature. The Thermotron was provided free-of-charge by ATD (Atmospheric Technology Division) for this investigation.

In fall 2000 each of six Geonor gauges (including one of the above) was placed inside a different windshield in anticipation of making snow measurements during winter 2002-2001. A field calibration-verification of each gauge was performed in November 2000. Two subsequent complete field calibration-verifications were performed, one in January 2002 and one in July 2002.

The purpose of a calibration-verification is to answer the question: Is there a sufficiently large difference between the observed response and response derived from factory coefficients to warrant a recalibration of a vibrating wire? The numerical value of "sufficiently large" has yet to be decided. Based on the results of the calibration-verifications, useful numerical values will be suggested.

In this paper we discuss performance and analysis of field calibration-verifications in Section 2, review previous laboratory calibration-

verifications in Section 3, and evaluate the stability of factory calibrations in Section 4. In Section 5 we show comparisons of liquid equivalent snowfall accumulations among 3 wires in a Geonor gauge from 5 snow events near Boulder, CO in 2002. We provide a comparison of rainfall rates between a Geonor gauge and state-of-the-art 2-dimensional video disdrometer in Section 6 and the summary and conclusions in Section 7. The Appendix provides a graphical presentation of results from all laboratory and field calibration-verifications.

2. FIELD CALIBRATION-VERIFICATION PROCEDURE AND RESULTS

The relationship between the depth of water (or liquid mixture) in a Geonor bucket and frequency of an attached vibrating wire is expressed through the quadratic calibration equation given by

$$P = A(f - f_0) + B(f - f_0)^2 \quad (1)$$

where f_0 is the frequency in Hz corresponding to an empty bucket, f is the frequency in Hz associated with precipitation P . The coefficients A and B are on the order of 10^{-2} cm Hz⁻¹ and 10^{-5} cm Hz⁻² when P is in cm. Coefficients A and B are determined at the factory by suspending known weights from each wire and fitting Eq.(1) to the observations. Null frequency f_0 is apparently determined by suspending a weight representative of all buckets and noting the output frequency. Geonor sells each vibrating wire with a unique A , B , and f_0 . Henceforth, all three quantities will be referred to as coefficients.

The approach taken to monitor the stability of a vibrating wire transducer was to place successive known weights in the bucket, calculate P (in a data logger) for each vibrating wire (hereafter referred to as simply wire), compare each value of P to the known weight converted to its equivalent depth of water, and derive a calibration error representative of the 3 sets of

Corresponding author address: Claude E. Duchon, School of Meteorology, Univ. of Oklahoma, Norman, OK 73019; email: cduchon@ou.edu

factory coefficients, one set for each wire. An example of a calibration-verification is shown in Fig. 1 for the Geonor gauge in the small Wyoming (sWyo) windshield. There is no effect of a windshield on a calibration-verification. The Geonor gauge in this example just happens to be located in the sWyo windshield, one of 6 windshields. Fig. 1(a) shows the differences between P (in mm) and the known weights (in mm) for each of the three wires and their average on the vertical axis plotted against the known accumulated weights. The calibration-verification was performed on 8 January 2002 using a set of 14 stainless steel disks ranging in weight from 797.5 g to 800.2 g and a base to support the disks with weight 401.7 g. As seen in Fig. 1(a) these weights yield an equivalent range in depth of water from 0 mm (empty-bucket) to 580 mm (base plus 14 weights). The weights were fabricated at the University of Oklahoma and will be referred to as the OU weights.

Prior to successively adding and removing weights the bucket and base were leveled. The addition and removal of weights explains why there are two curves for each wire. The black curve in Fig. 1(a) is the average of the three curves of the individual wires. One notices immediately that even with no accumulation (empty bucket) the differences along the vertical axis for each wire are displaced from each other. This is typical behavior and may be, in part, a consequence of using a bucket whose weight is different than the bucket weight employed in the factory calibration of f_0 .

The divergence of differences from the individual wires with increasing accumulated weight can be much greater than shown in Fig. 1(a). In Fig. 2(a), the format of which parallels Fig. 1(a), a calibration-verification of the same wires was made with a different set of known weights 14 months earlier. The divergence of differences is considerably greater. Nevertheless, the average of the three wires differs by less than 1-1/4 mm from the average in Fig. 1(a) throughout the 0 to 600 mm accumulation. Fig. 2(a) indicates the mass of the weights was increasingly non-uniformly distributed with increasing number of weights. The similarity of the two average curves shows that having a truly uniform mass distribution is not necessary to obtain a valid calibration-verification.

The next step in analyzing the data from a calibration-verification is to model the average

difference curve with a low order polynomial. Fig. 1(b) shows that a 2nd degree polynomial provides the optimal fit. By "optimal" is meant that the increase in the value of R^2 (square of the correlation coefficient) is small so that a higher order polynomial is unwarranted. The highest order polynomial chosen among all calibration-verifications was 3. The value of 0.82 for R^2 means that the fitted curve and the average curve have 82% of their variance in common. If the two curves had been coincident, the value of R^2 would have been unity. Because the goal of a calibration-verification is calibration error assessment, the final step is to differentiate the fitted polynomial. The left-hand vertical axis in Fig. 1(c) is the slope of polynomial multiplied by 10 to yield calibration error in mm per 10 mm precipitation. The nominal depth of a convective rain shower across the Southern Plains is 10 mm (about 0.4 in). The range in calibration error per 10 mm accumulation varies linearly from about 0.01 mm for bucket accumulations under 100 mm to around -0.04 mm for bucket accumulations greater than 500 mm. The right-hand vertical axis is the calibration error in percent obtained by multiplying the slope of the polynomial in Fig. 1(b) by 100. Thus the parallel range in calibration error corresponding to the range in calibration error per 10 mm is from 0.1% to -0.4%. It should be pointed out that had one chosen to determine calibration error per 20 mm accumulation, say, the error in mm would be twice that for a 10 mm accumulation, while the calibration error in percent would remain unchanged.

The calibration errors obtained in Figs. 1(c) and 2(c) are associated with a calibration-verification only and should not be considered operational errors. Errors associated with evaporation from the interior wall of the collection cylinder and undercatch due to wind, as examples, are part of normal precipitation measurement but play no part in a calibration-verification. That a smooth curve is fitted to a noisy curve as in Fig. 1(b) is based on the notion that an ideal calibration-verification would yield, in fact, a smoothly changing average curve. Presumably, the noise is the sum of frequency round-off error in the data logger, resolution and repeatability errors in the vibrating wire transducers, stray radio noise, and, perhaps, other error sources. These errors would be part of the normal measurement of precipitation.

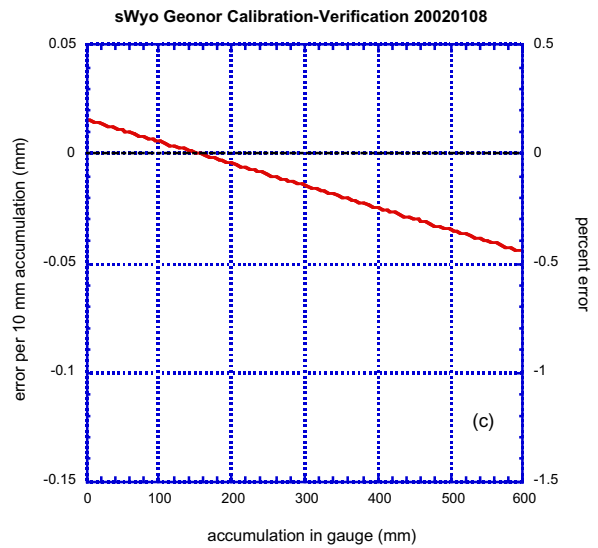
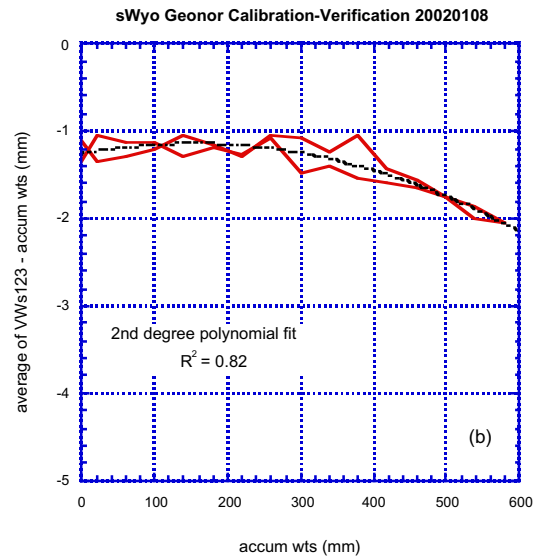
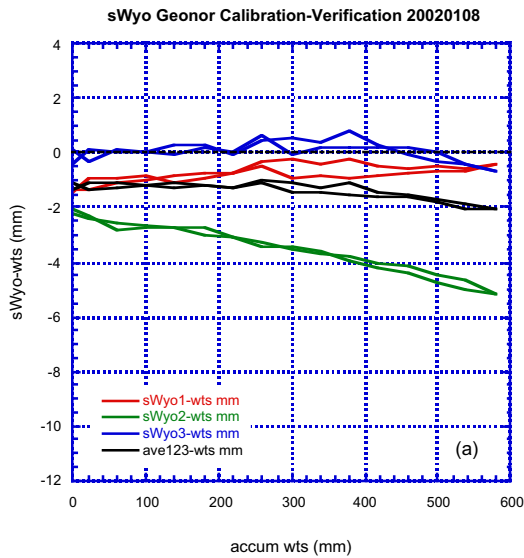


Fig. 1 Differences between individual wires and accumulated weights and average differences versus accumulated weights are shown in (a). The minimum least-squares 2nd degree polynomial fit to the average differences is shown in (b) and the slope of the fitted polynomial in (b) in terms of calibration error per 10 mm accumulation and calibration error in percent is shown in (c). Data are from calibration-verification 8 January 2002.

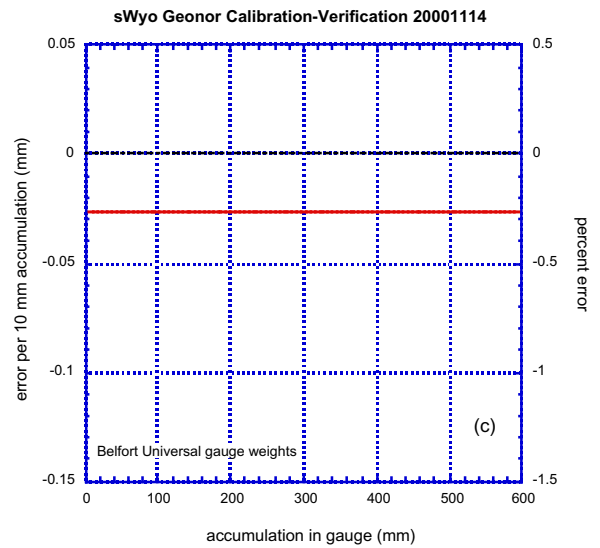
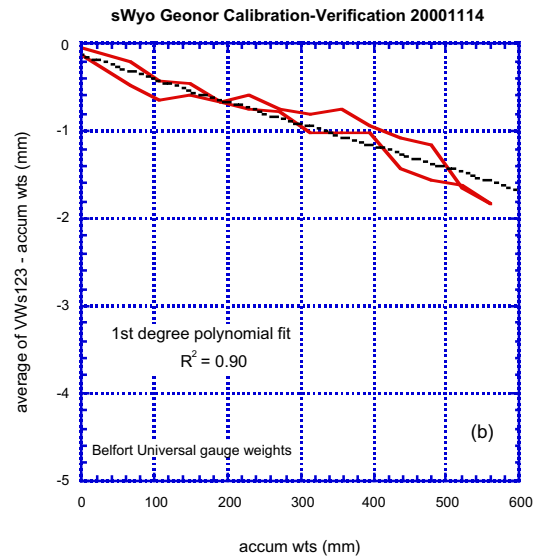
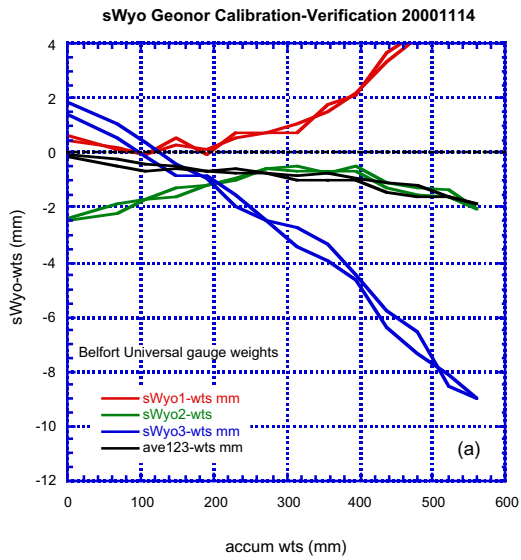


Fig. 2 Same as Fig. 1 except results apply to the calibration-verification performed 14 November 2000 in which the Belfort weights were used.

Results from the third and latest calibration-verification of the Geonor gauge in the sWyo are shown in Fig. 3. The trends in differences for individual wires in Fig. 3(a) are different than those in the previous calibration-verifications; however, the average curves among the three calibration-verifications are quite similar, especially the later two in which the same set of weights was employed. Thus the calibration error curves in Figs. 1(c) and 3(c) are also quite similar. With the exception of the part of the curve in Fig. 3(c) for accumulations greater than 500 mm, all three calibration error curves lie within $\pm 0.5\%$.

Figs. 4 and 5, respectively, document the results of the calibration-verifications performed 8 January and 9 July 2002 of the Geonor gauge in the ndAlt (new double Alter) windshield, the only calibration-verifications with this combination of wires. It is remarkable that the two independent calibrations, except for using the same weights, yield such similar results. There is no particular position of a weight on the spindle – a weight is simply selected from the ordered stack of weights and placed over the spindle on top of the previous weight. In each figure the curve of average differences decreases noticeably with increasing accumulation. Similarly, the polynomials fitted to the curves of average differences in Figs. 4(b) and 5(b) are both 2nd degree with $R^2 > 0.95$. For accumulations greater than about 400 mm, the absolute calibration errors in Figs. 4(c) and 5(c) exceed 1%. Figs. 4(a) and 5(a) indicate there may be a problem with wire 2. It appears that variations between individual difference curves that result from non-uniform distribution of mass in the bucket are overwhelmed by the systematic downward trend in wire 2, suggesting a laboratory recalibration of wire 2 is warranted.

3. LABORATORY CALIBRATION-VERIFICATION PROCEDURE AND RESULTS

As mentioned in the Introduction, two Geonor gauges, each with 3 wires, were provided to NCAR by USCRN in spring 2000 for testing. This type of gauge had been used earlier in field studies at Marshall test facility but had not been subjected to calibration-verification using both water weights and metal weights and over a range of temperatures. The goals of the laboratory tests were to determine whether metal weights produced results different than water weights and

whether the temperature during a calibration-verification impacted the results. The calibration-verification procedure in the laboratory was essentially the same as in the field except that weights were placed in the bucket with the gauge case (or shell) removed.

The results of the laboratory calibration-verifications are presented in Figs. A.1. – A.12 in the Appendix. By comparing the (a) panels in the figures it is apparent that use of water weights resulted in smoother difference curves than did use of the metal weights. However, curves of the averages of the three wires seem to be essentially independent of type of weight. The two calibration-verifications at about 0 C and -16 C (Figs. A.5(a), A.6(a), A.11(a), A.12(a)) appear to be reasonably consistent with the previously observed negative coefficient of temperature sensitivity. That is, curves of the average of the differences tend to be higher the colder the temperature. Of course, the calibration-verifications below freezing were performed using metal weights. Inserting the weights was awkward because the gauges were in the Thermotron. To add weights to the buckets required opening and closing the chamber door and the need for gloves to handle the cold metal.

The calibration error curves in the (c) panels of Fig. A.1 – A.12 do not show a preferred dependence on either temperature or type of weight. In practically all calibration-verifications, most of each calibration error curve lies within the -0.5 to 0.5% range. The largest absolute calibration errors occur above 500 mm accumulation for the two colder temperatures as seen in Figs. A.5(c), A.6(c), A.11(c), and A.12(c). After the period of testing ended in August 2000, only one of the two gauges was retained and used in subsequent field studies at the Marshall test facility. The wires in this gauge were separated so that their unique combination no longer could be tracked.

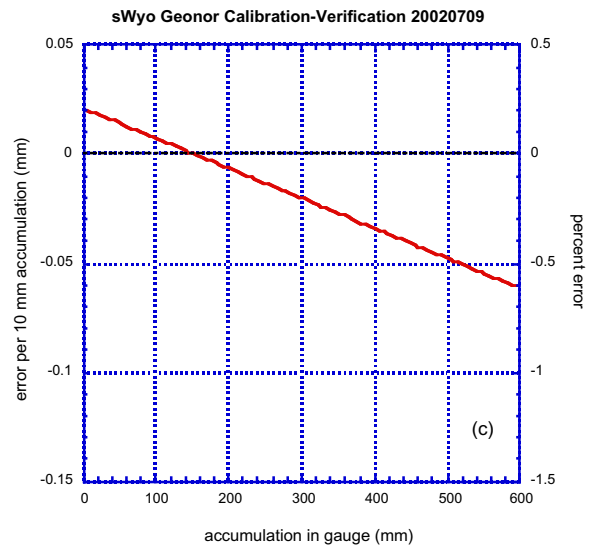
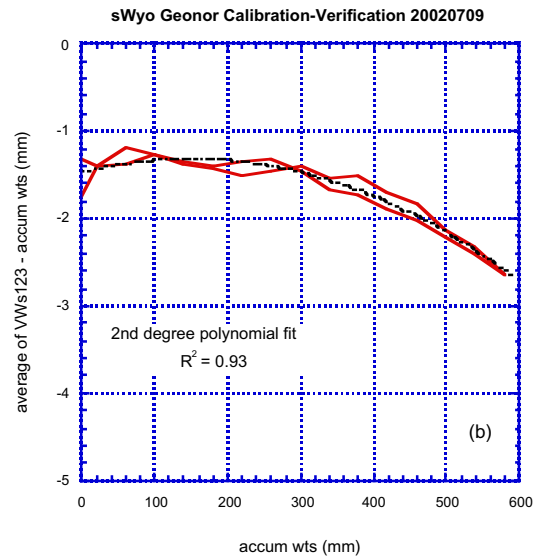
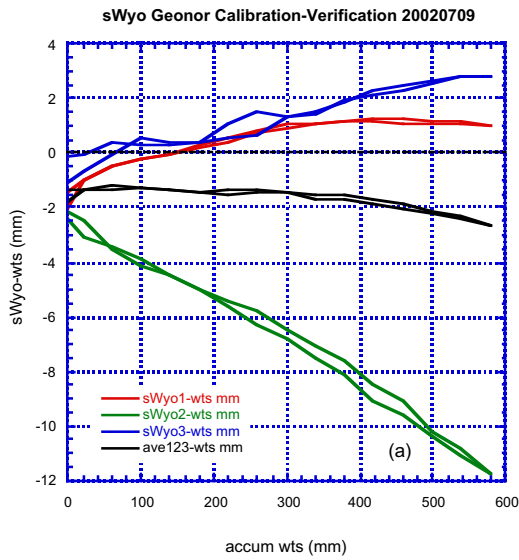


Fig. 3 Same as Fig. 1 except results apply to the calibration-verification performed 9 July 2002.

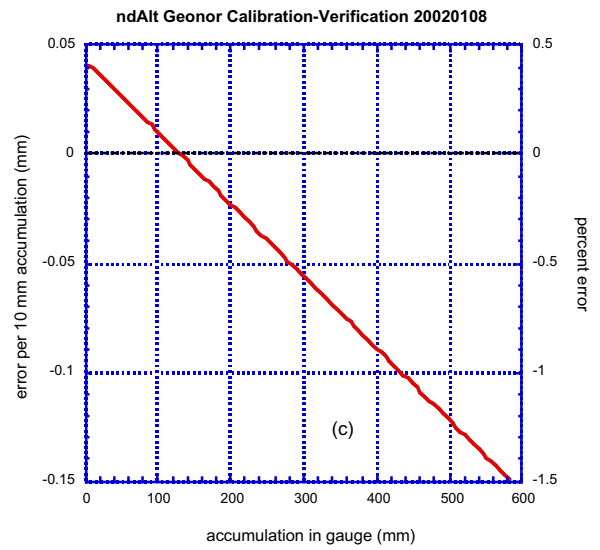
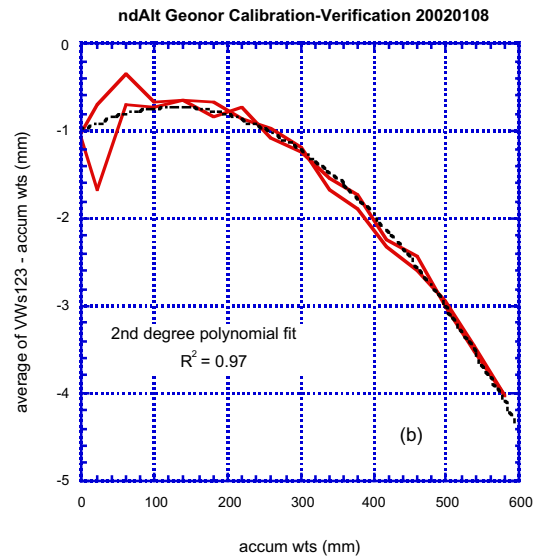
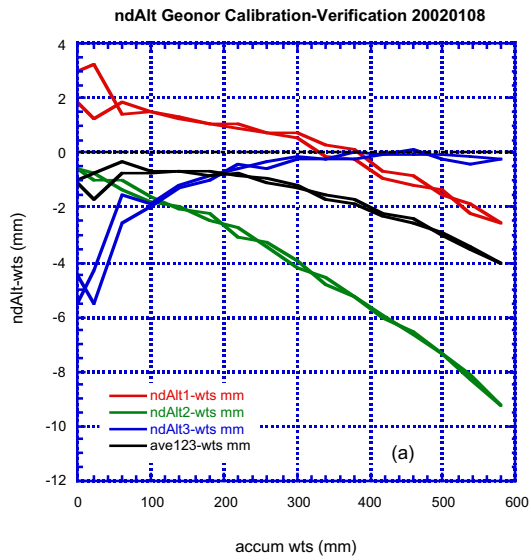


Fig. 4 Same format as Fig. 1 except this Geonor gauge is in the ndAlt windshield.

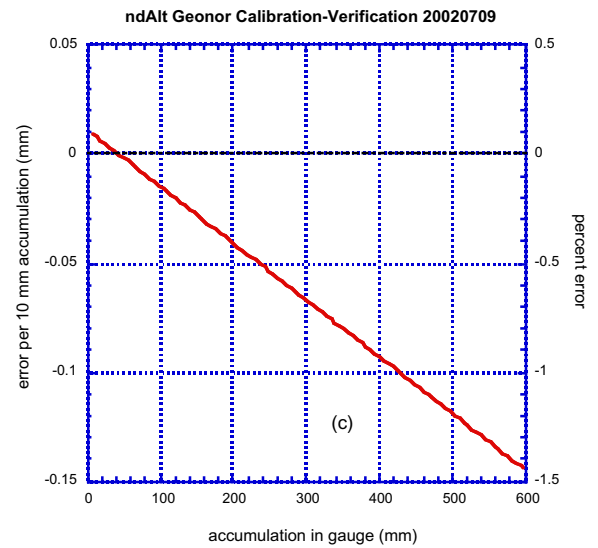
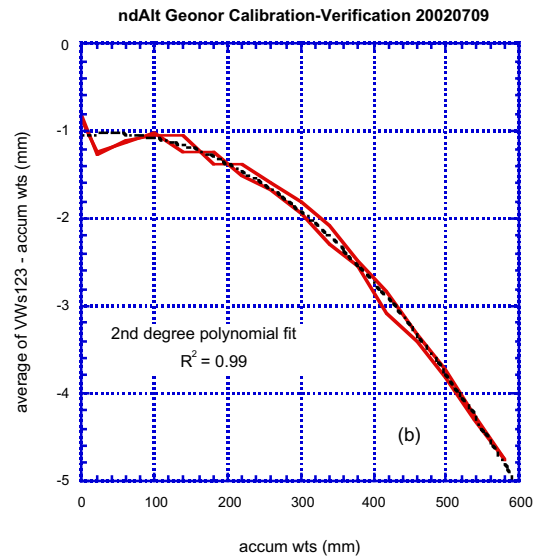
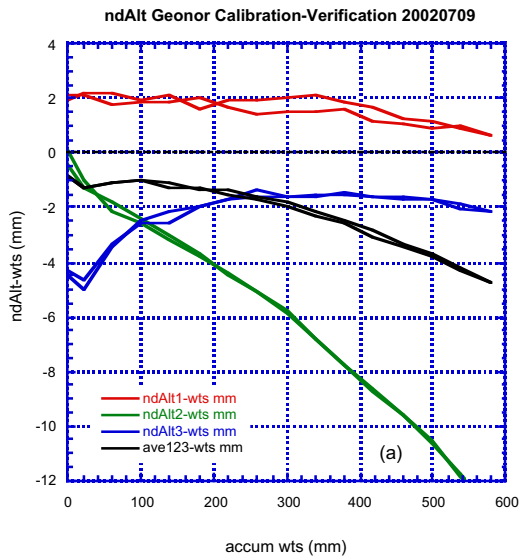


Fig. 5 Same as Fig. 4 except the calibration-verification was performed 9 July 2002.

4. ASSESSMENT OF STABILITY OF CALIBRATIONS

Tables 1-10 provide a systematic way of observing the change in range of calibration error in percent with time for each set of 3 wires. The left-hand column in each table shows time increasing downward with the related range in calibration error in the right-hand column. Apart from the exceptions noted in Sections 2 and 3, all calibration errors lies within +/-1% and many are

within +/-0.5%. In Tables 1 and 2 the largest calibration errors occur with the colder temperatures. The large errors in Table 10 have already been discussed.

These tables show that, on the whole, during the 20-month period from November 2000 to July 2002 the calibration errors are small and, as a consequence, do not show easily identifiable trends. As indicated earlier, the exception in Table 10 deserves attention.

Summary of Laboratory and Field Calibration-Verifications of Vibrating Wire Transducers Used in Geonor T-200B Precipitation Gauges

Table 1 Serial numbers: 12700 12900 13000

Date	Mean Temperature (C)	Type of Weights	Degree of Polynomial Fit	R ²	Range in Percent Calibration Error: 0 to 600 mm
23 March 2000	23	water	2	0.86	-0.2 to 0.2
24 March 2000	23	water	2	0.80	-0.2 to 0.2
17 August 2000	23	Belfort	2	0.94	-0.5 to 0.2
18 August 2000	23	water	2	0.99	-0.4 to 0.0
28 August 2000	-16	Belfort	3	0.73	-0.7 to 0.1
29 August 2000	0	Belfort	3	0.77	-0.7 to 0.1

Table 2 Serial numbers: 13100 13200 13300

Date	Mean Temperature (C)	Type of Weights	Degree of Polynomial Fit	R ²	Range in Percent Calibration Error: 0 to 600 mm
23 March 2000	23	water	3	0.88	-0.6 to 0.3
24 March 2000	23	water	3	0.95	-0.5 to 0.3
17 August 2000	23	Belfort	3	0.24	-0.5 to 0.1
18 August 2000	23	water	2	0.90	-0.3 to 0.6
28 August 2000	-16	Belfort	3	0.73	-1.1 to 0.4
29 August 2000	0	Belfort	3	0.79	-1.0 to 0.3

Table 3 Serial numbers: 23000 23100 23200 (in DFIR)

Date	Mean Temperature (C)	Type of Weights	Degree of Polynomial Fit	R ²	Range in Percent Calibration Error: 0 to 600 mm
14 November 2000	21	Belfort	1	0.92	-0.3
7 January 2002	13	OU	1	0.88	-0.2
9 July 2002	28	OU	1	0.96	-0.3

Table 4 Serial numbers: 13000 13100 13200 (in sDFIR)

Date	Mean Temperature (C)	Type of Weights	Degree of Polynomial Fit	R ²	Range in Percent Calibration error: 0 to 600 mm
14 November 2000	21	Belfort	3	0.85	-0.1 to 0.0
7 January 2002	13	OU	3	0.54	-0.8 to 0.1
9 July 2002	29	OU	3	0.85	-0.8 to 0.0

Table 5 Serial numbers: 12700 12900 34498 (in sWyo)

Date	Mean Temperature (C)	Type of Weights	Degree of Polynomial Fit	R ²	Range in Percent Calibration Error: 0 to 600 mm
14 November 2000	22	Belfort	1	0.90	-0.3
8 January 2002	17	OU	2	0.82	-0.5 to 0.2
9 July 2002	31	OU	2	0.93	-0.6 to 0.2

Table 6 Serial numbers: 27300 27400 27500 (in sAlt)

Date	Mean Temperature (C)	Type of Weights	Degree of Polynomial Fit	R ²	Range in Percent Calibration Error: 0 to 600 mm
29 November 2000	21	Belfort	3	0.92	-0.8 to -0.1
8 January 2002	16	OU	3	0.61	-0.2 to 0.5
9 July 2002	32	OU	3	0.68	-0.2 to 0.4

Table 7 Serial numbers: 23300 23400 23500 (in dAlt)

Date	Mean Temperature (C)	Type of Weights	Degree of Polynomial Fit	R ²	Range in Percent Calibration Error: 0 to 600 mm
14 November 2000	21	Belfort	1	0.93	-0.2

Table 8 Serial numbers: 23300 11301 11401 (in dAlt)

Date	Mean Temperature (C)	Type of Weights	Degree of Polynomial Fit	R ²	Range in Percent Calibration Error: 0 to 600 mm
7 January 2002	11	OU	2	0.82	-0.4 to 0.2
9 July 2002	30	OU	1	0.97	-0.3

Table 9 Serial numbers: 24898 29298 29198 (in Wyo)

Date	Mean Temperature (C)	Type of Weights	Degree of Polynomial Fit	R ²	Range in Percent Calibration Error: 0 to 600 mm
15 November 2000	22	Belfort	1	0.91	-0.4

Table 10 Serial numbers: 29198 26000 29298 (in ndAlt)

Date	Mean Temperature (C)	Type of Weights	Degree of Polynomial Fit	R ²	Range in Percent Calibration Error: 0 to 600 mm
8 January 2002	16	OU	2	0.97	-1.6 to 0.4
9 July 2002	29	OU	2	0.99	-1.4 to 0.1

5. COMPARATIVE ACCUMULATIONS IN SNOW EVENTS

In this section we provide examples of 1-minute liquid-equivalent snowfall accumulations from one among 6 Geonor gauges that were used to measure snowfall during winter 2001-2002 at NCAR's Marshall Test Facility south of Boulder, CO. Each gauge contained adequate antifreeze covered by a thin oil layer so that snow melted as it entered the liquid in the bucket. In addition, the orifice of each gauge was heated to prevent accumulation of wet snow on the orifice. Each of the 6 gauges was located in a windshield of different design. The gauge discussed here was located in a WMO windshield standard, the double fence intercomparison reference (DFIR). It was selected because one of its 3 wires shows abnormal behavior of the kind that is easy to detect visually but would take some skill to flag in an operational error identification scheme. Detection would be strongly aided using the other two wires.

Fig. 6 shows the results from 5 snow events. Common to each panel is the time axis – one UTC day. The units of each vertical axis are mm but the range varies to maximize resolution. Fig. 6(a) shows the snowfall on 10 January commencing at minute 360 and ending at minute 780 with the totals from each wire shown in the box in the lower right-hand part of the panel along with the maximum difference in accumulation among the 3 wires at the termination of the snow event. As shown in the upper left of the panel, the 3 m air temperature varied from -0.5 to -1.5 C, the former value at the beginning of the snowfall and the latter at the end. In practically all cases (including cases not discussed here), the warmest temperature occurred at the beginning of the snow event and the coldest temperature at the end. The accumulation associated with a particular snowfall was determined by noting the accumulation in the bucket at the beginning of the snowfall and subtracting it from each subsequent 1-minute accumulation. The initial accumulation for each wire is given in the box in the middle right-hand part of the panel.

It can be seen that wires 1 and 2 track each other very closely in Fig. 6(a) and wire 3 begins to diverge at around the midpoint of the event. What is most notable is the irregularity in the trace of wire 3 after the end of the event. Clearly, there is

a problem with wire 3 or its signal conditioning electronics.

Fig. 6(b) shows the total or actual accumulations for each wire for the snow event on 25 February. The same kind of irregular fluctuations can be seen again in wire 3, particularly before and after the snow event which began about minute 400 and ended at minute 960. Fig. 6(c) shows accumulations from wires 1 and 2 for the same snow event. The difference in liquid-equivalent accumulation is 0.21 mm. Had wire 3 been included, the maximum difference would have increased to about 0.30 mm.

The remaining panels show accumulations for 3 snow events in March with event totals ranging from 3.5 mm to 21 mm. In each event wires 1 and 2 track each other quite well although in each they diverge with increasing accumulation. Wire 3 also tracks wires 1 and 2 but shows unsteadiness particularly when the snowfall has ended.

In summary, the 3 wires track each quite closely during time of precipitation, but wire 3 exhibits odd behavior over the two-month period. Wire 3 should have been replaced by a new wire to determine whether it or the signal conditioning electronics was defective.

The differences between the maximum and minimum liquid-equivalent snow event totals among the 3 wires vary from 0.2 to 0.7 mm (0.01 to 0.03 in) over the 5 events. In fact, the difference of 0.72 mm in panel (d) is the largest difference among all 6 Geonor gauges for the 5 events. Typically, differences are less than 0.2 mm (about 0.01 in). Since differences between any two wires tend to be systematic, we should expect the differences between maximum and minimum accumulation to be proportional to snow event total, as observed by comparing maximum differences with event totals in Fig. 6.

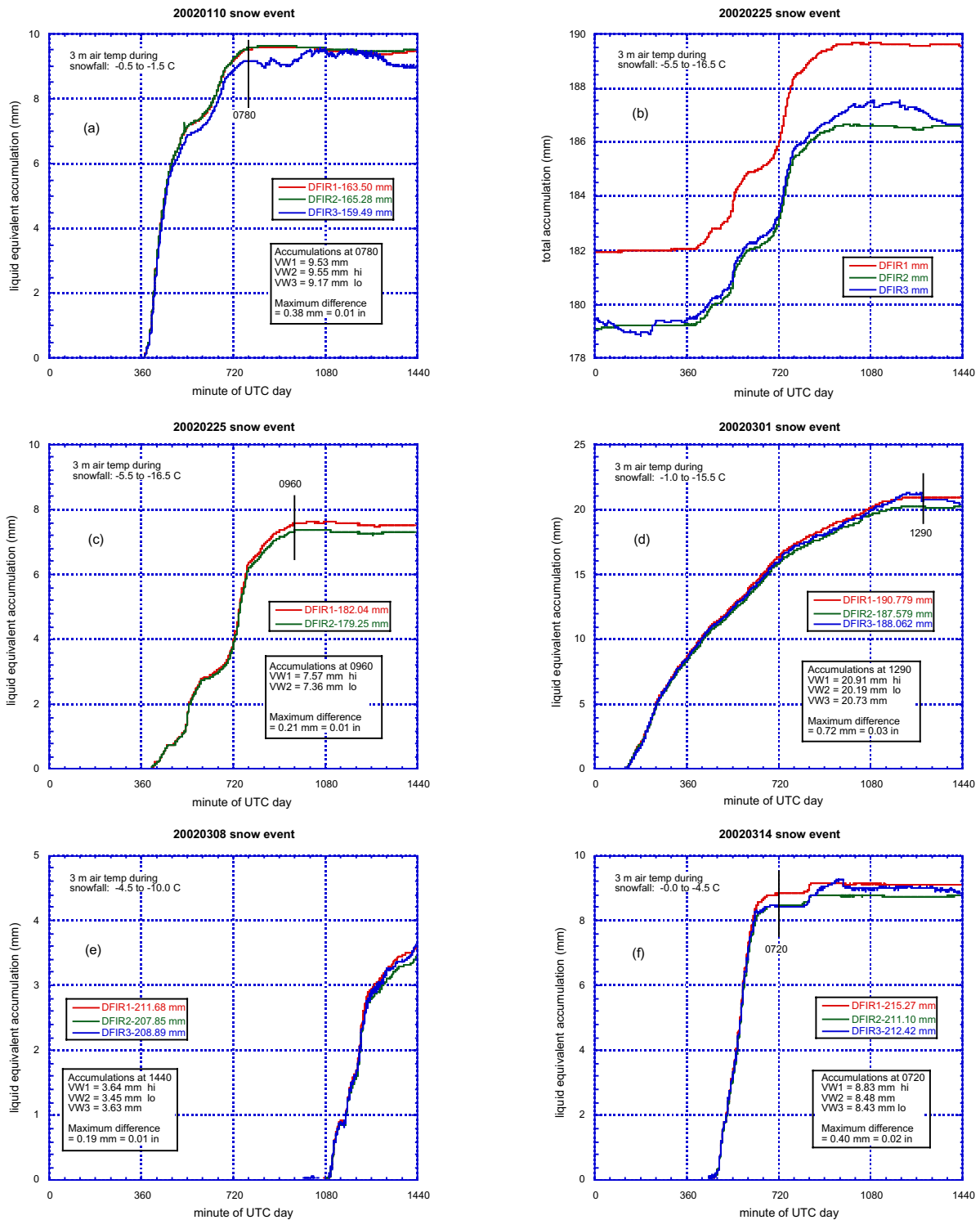


Fig. 6 Plots of liquid equivalent snowfall accumulations for the 3 vibrating wires in the Geonor gauge in the DFIR windshield for 5 snow events in 2002. (a) Snow event accumulations for 10 January. (b) Accumulations in the bucket for 25 February. (c) Snow event accumulations for wires 1 and 2 for 25 February. (d), (e), (f) Snow event accumulations for 1 March, 8 March, and 14 March.

6. COMPARISON OF RAINFALL RATES FROM A GAUGE AND A DISDROMETER

Comparison of rainfall rates from a 3-wire Geonor gauge and a 2-dimensional video disdrometer (manufactured by Joanneum Research, Graz, Austria) were made from May 2001 to July 2002. Both the gauge and the disdrometer were located at an open field site (no obstructions) in north Norman, OK. Both instruments were positioned in pits such that the orifice of each was about 2 cm above a fabric filter attached to a grill that surrounded the orifice. The filter served to reduced drop splash. Rain passed through the filter and grill into the pit where it was pumped to the surface and away from the pit. The pits were separated by about 5 m.

One-minute rainfall rates were obtained, respectively, by summing the volumes of the 1-minute distributions of drop sizes measured by the 2-dimensional video disdrometer (hereafter, 2dvd) and computing the difference between successive averages of 1-minute accumulations from the 3 wires in the Geonor gauge. Rainfall rates from individual wires in the Geonor were much noisier.

Fig. 7 is a comparison of 1-minute rainfall rates over a 4-hour period on 23 January. The 1-minute fluctuations in the Geonor rainfall rates are due to noise inherent in accumulation measurements. In the case of the 2dvd, when no rain is occurring, the rainfall rate is set to zero. The curves are displaced in time from each other by 2 minutes for ease in viewing them. In this context there is a remarkable similarity between the two independent sources of rainfall rate. This is especially noteworthy because during the two peak rainfall rate periods the 5-minute average 10-m wind speed was as high as 8 ms^{-1} . A recent study showed that undercatch due to a shadowing effect by the orifice of the 2dvd increases as the 5-minute average 10-m wind speed increases from 5 ms^{-1} .

In summary, the comparison in Fig. 7 shows that the relatively inexpensive Geonor gauge (with respect to the 2dvd) can provide a very good estimate of rainfall rate. It should be a good instrument for developing rainfall rate and liquid-equivalent snowfall rate climatologies.

20020123 rain event

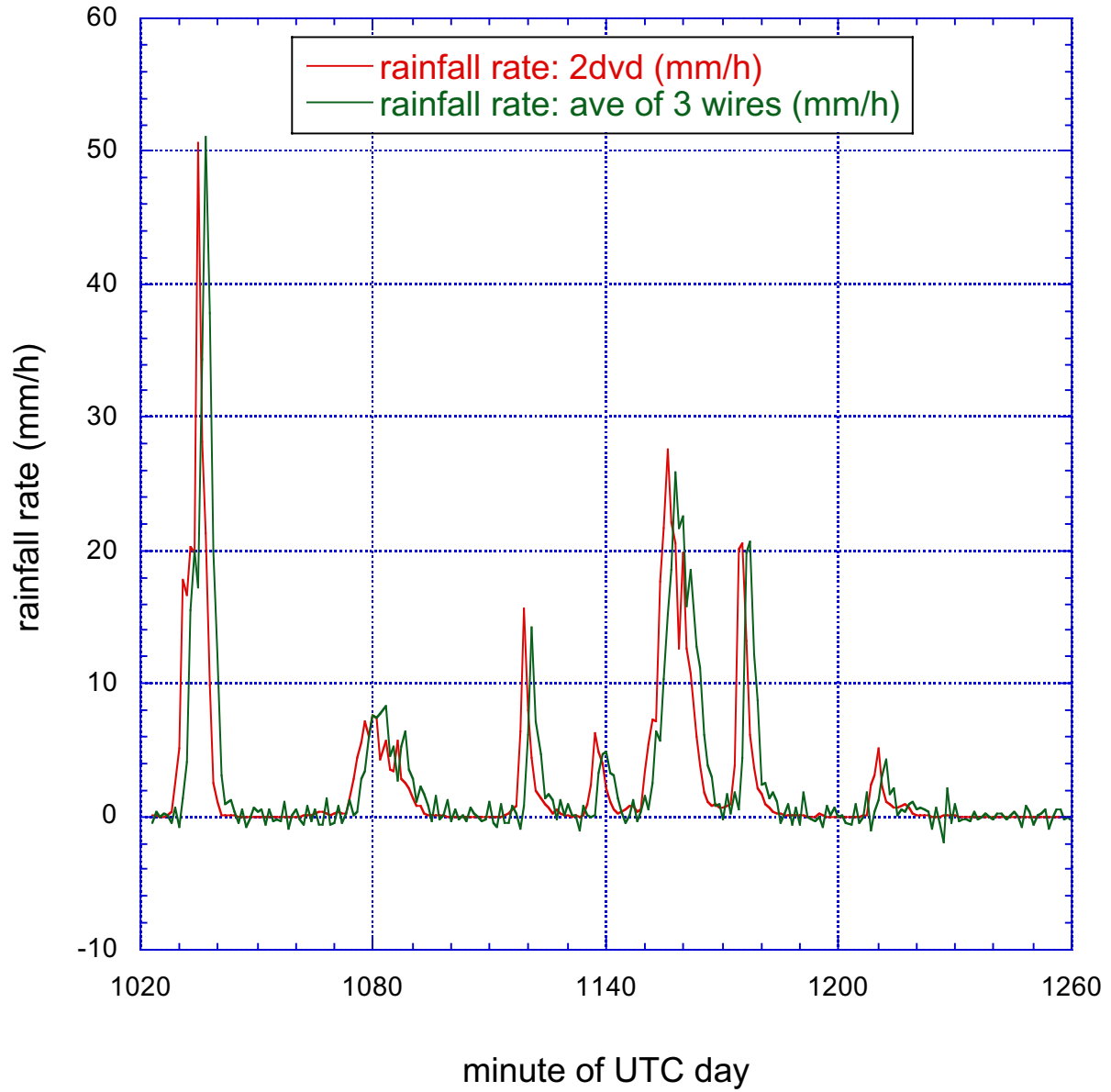


Fig. 7 Comparison of rainfall rates from a Geonor rain gauge and a 2-dimensional video disdrometer. The two curves are offset in time to facilitate their comparison.

7. SUMMARY AND CONCLUSIONS

Over the 28-month period from March 2000 to July 2002 30 laboratory and field calibration-verifications were performed on 22 vibrating wires at the NCAR Foothills Lab and NCAR's Marshall field site. The main purpose was to observe the stability of factory calibrations of Geonor gauges, that is, watch for significant systematic changes in calibration coefficients.

In addition to monitoring calibration stability over a 5-month period, additional goals of the laboratory calibration-verifications were to determine the sensitivity of the calibration coefficients to temperature and the impact of using metal weights instead of water weights. The results of the laboratory test are:

- (1) There was no evidence of significant systematic changes in the values of coefficients over this time period.
- (2) There appeared to be a small dependence of the values of coefficients on temperature based on an increase in calibration error at temperatures from 0 C to -16 C relative to the calibration error at room temperature.
- (3) The use of water weights provided a more uniform distribution of mass in the bucket than metal weights (at least relative to those that were used). One disadvantage of using water weights is that a calibration-verification can be performed only for increasing weight.

The field calibration-verifications were performed over the 20-month period November 2000 to July 2002 and covered the temperature range 11 to 30 C. Metal weights were used exclusively. The results of the field tests are:

- (1) Using the average of three vibrating wires, practically all field calibration errors were within +/-1% and most within +/-0.5%. There was evidence that one of the wires in the gauge that exceeded 1% calibration error should be recalibrated in a laboratory.
- (2) Apart from the vibrating wire above, there was no evidence for significant changes in calibration coefficients, based on using the

average of three wires to assess calibration error.

Because 19 of 20 wires with at least two calibration-verifications showed no significant drift in their calibration coefficients over periods ranging from 6 months to 28 months, it can be concluded that the Geonor vibrating wire transducers show good stability.

We presented examples of the performance of a Geonor precipitation gauge for 5 snow events near Boulder, CO. We showed an advantage of using 3 wires as opposed to 1 or 2. One of the 3 wires exhibited erratic fluctuations, particularly when there was no precipitation. A cleverly designed algorithm that involves intercomparisons among the 3 wires should enable operational detection of improper behavior of a wire.

A comparison of rainfall rates from a Geonor gauge and a 2-dimensional video disdrometer at Norman, OK showed very close correspondence between their time series. One implication is that the modestly priced Geonor gauge can be used to accurately estimate rainfall rates for meteorological and climatological needs.

Acknowledgments

We acknowledge and appreciate free use of NCAR's Marshall field site and foothills laboratory facilities, especially the Thermotron. We appreciate, also, the cooperation of members of the NCAR staff.

Appendix

Results from all Laboratory and Field Calibration-Verifications

The format for all figures in the Appendix is the same. Panel (a) in the upper left of a figure provides curves of the differences between individual wires and accumulated weights and their average versus accumulated weights. Panel (b) in the upper right of the figure shows curve of the average of the differences in panel (a) again and the minimum least-squares polynomial fitted to the curve. The goodness of the fit is given by the value of R^2 , the magnitude of the variance in common between the curve and polynomial. The slope of the fitted polynomial in (b) in terms of calibration error per

10 mm accumulation and percent error are shown in panel (c) in the lower right of the figure. Serial numbers for the wires are given in Table 1 in the main text.

As noted in the main text and in Tables 1-10, there are sometime only 1 or 2, instead of 3, field calibration-verifications. The reason is that 1 or 2 wires in a given gauge were replaced by other wires. This occurred twice, once when two wires in the dAlt windshield were replaced and once when the gauge in the Wyoming was placed in the ndAlt windshield in which case one wire was replaced.

List of Figures

Laboratory calibration-verifications (corresponding to Tables 1 and 2 in text)

A.1	23 March 2000	wires 1, 2, 3	water weights	average T = 23 C
A.2	24 March 2000	wires 1, 2, 3	water weights	average T = 23 C
A.3	17 August 2000	wires 1, 2, 3	metal weights	average T = 23 C
A.4	18 August 2000	wires 1, 2, 3	water weights	average T = 23 C
A.5	28 August 2000	wires 1, 2, 3	metal weights	average T = -16 C
A.6	29 August 2000	wires 1, 2, 3	metal weights	average T = 0 C
A.7	23 March 2000	wires 4, 5, 6	water weights	average T = 23 C
A.8	24 March 2000	wires 4, 5, 6	water weights	average T = 23 C
A.9	17 August 2000	wires 4, 5, 6	metal weights	average T = 23 C
A.10	18 August 2000	wires 4, 5, 6	water weights	average T = 23 C
A.11	28 August 2000	wires 4, 5, 6	metal weights	average T = -16 C
A.12	29 August 2000	wires 4, 5, 6	metal weights	average T = 0 C

Field calibration-verifications (corresponding to Tables 3 –10 in text)

A.13	14 November 2000	Geonor gauge in DFIR	Belfort weights
A.14	7 January 2002	Geonor gauge in DFIR	OU weights
A.15	9 July 2002	Geonor gauge in DFIR	OUweights
A.16	14 November 2000	Geonor gauge in sDFIR	Belfort weights
A.17	7 January 2002	Geonor gauge in sDFIR	OU weights
A.18	9 July 2002	Geonor gauge in sDFIR	OUweights
A.19	14 November 2000	Geonor gauge in sWyo	Belfort weights
A.20	8 January 2002	Geonor gauge in sWyo	OU weights
A.21	9 July 2002	Geonor gauge in sWyo	OUweights
A.22	29 November 2000	Geonor gauge in sAlt	Belfort weights

A.23	8 January 2002	Geonor gauge in sAlt	OU weights
A.24	9 July 2002	Geonor gauge in sAlt	OUweights
A.25	14 November 2000	Geonor gauge in dAlt	Belfort weights
A.26	7 January 2002	Geonor gauge in dAlt	OU weights
A.27	9 July 2002	Geonor gauge in dAlt	OUweights
A.28	15 November 2000	Geonor gauge in Wyo	Belfort weights
A.29	8 January 2002	Geonor gauge in ndAlt	OU weights
A.30	9 July 2002	Geonor gauge in ndAlt	OUweights

* * * * *

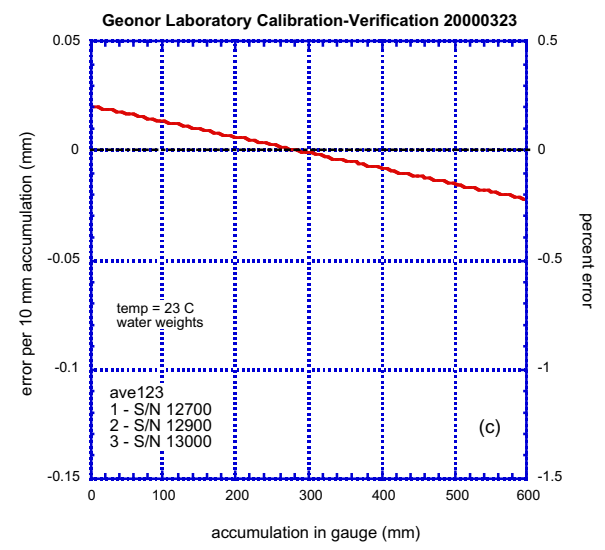
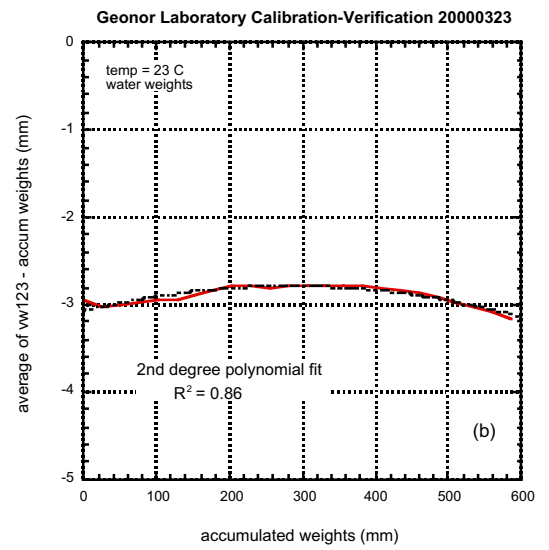
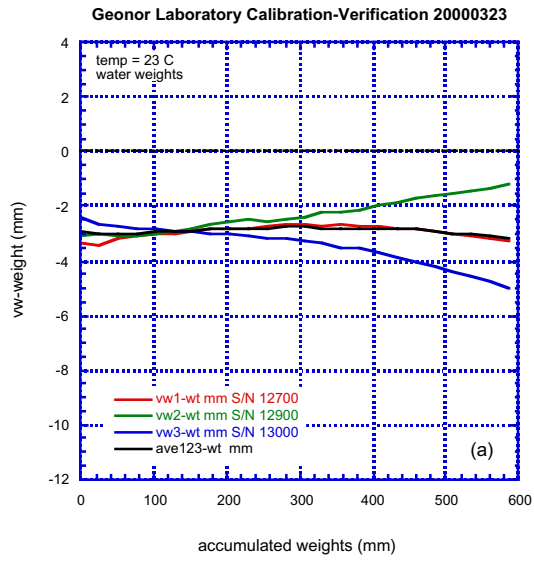


Fig. A.1

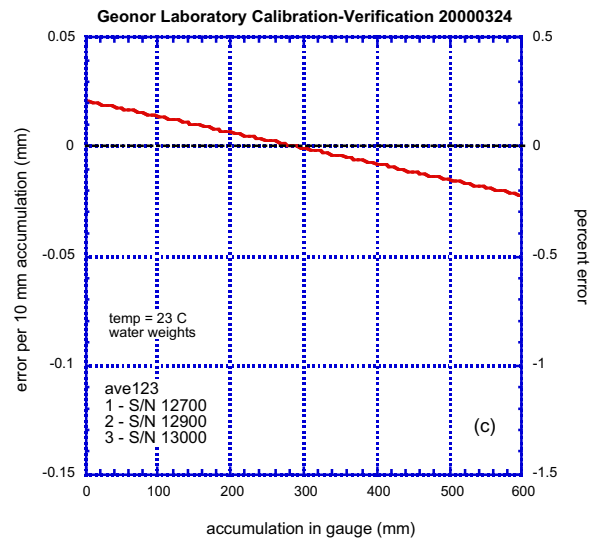
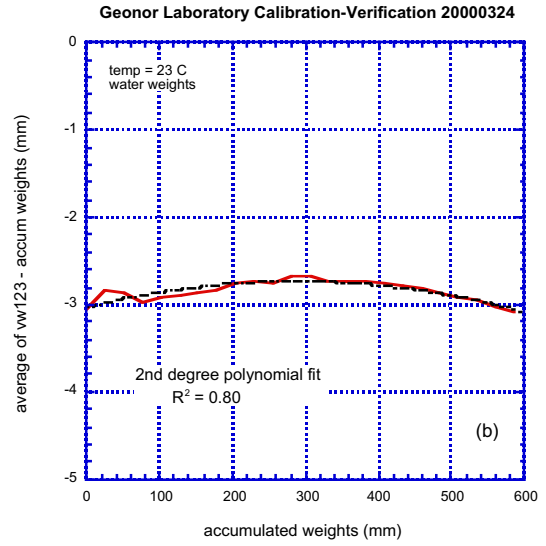
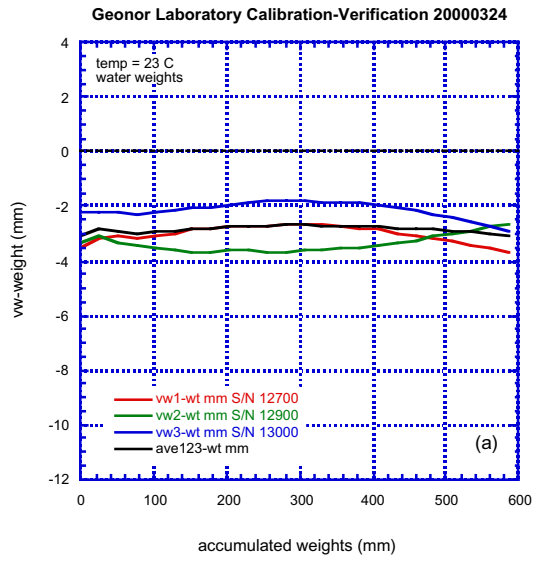


Fig. A.2

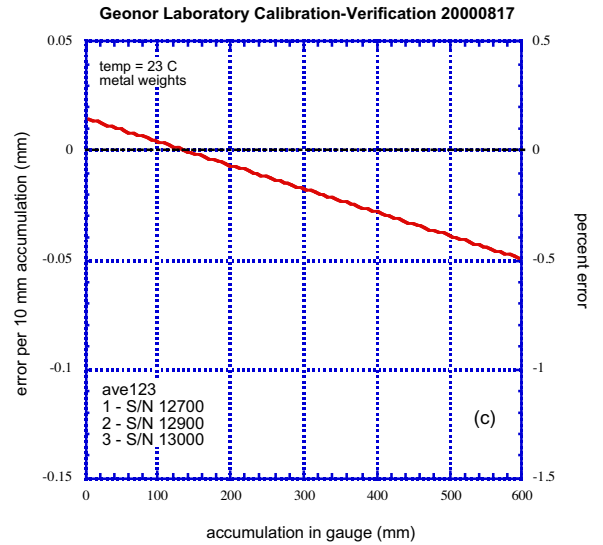
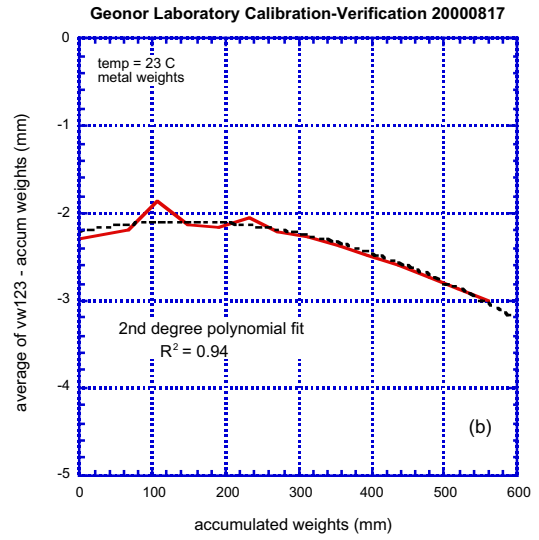
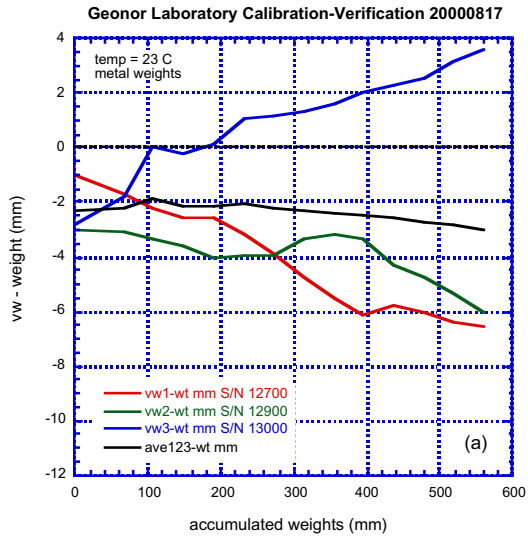


Fig. A.3

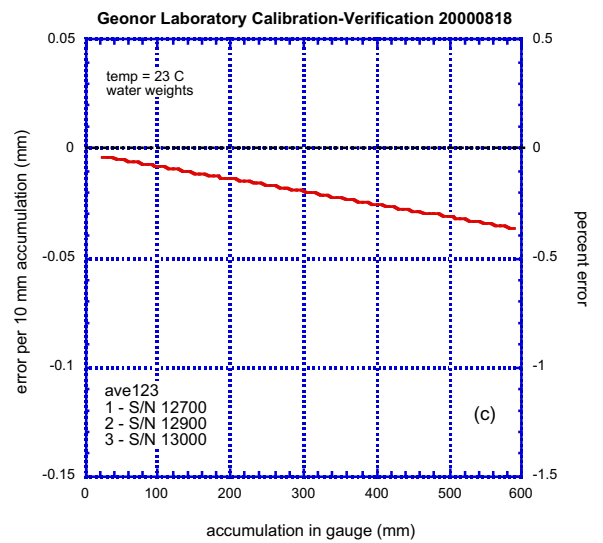
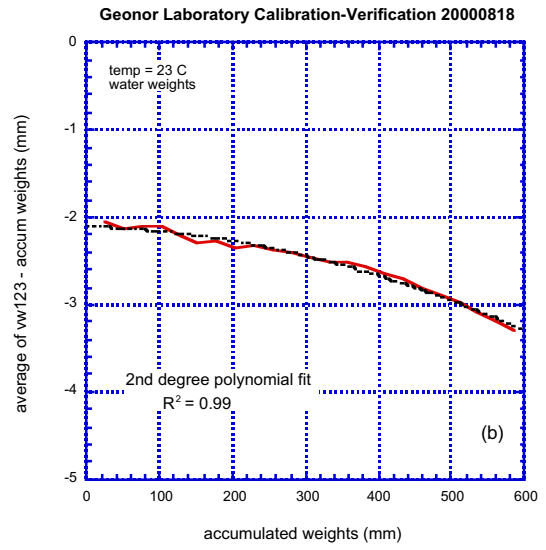
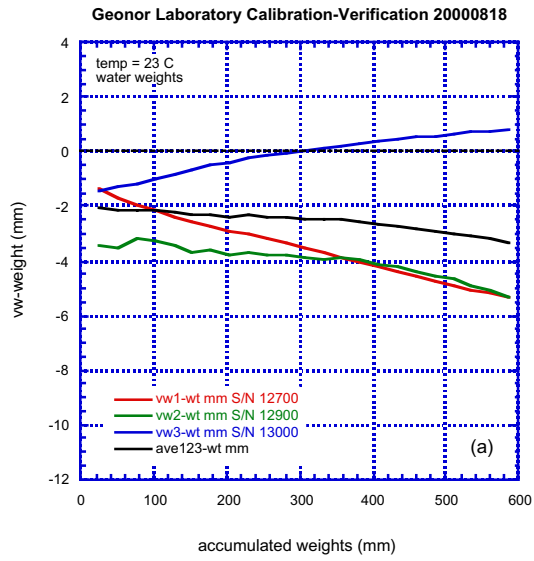


Fig. A.4

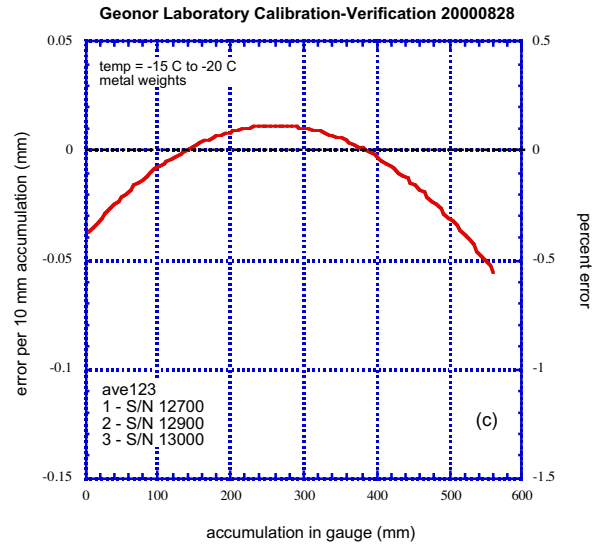
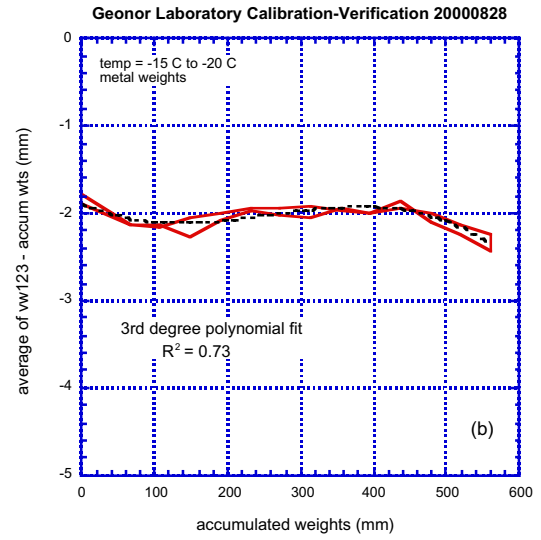
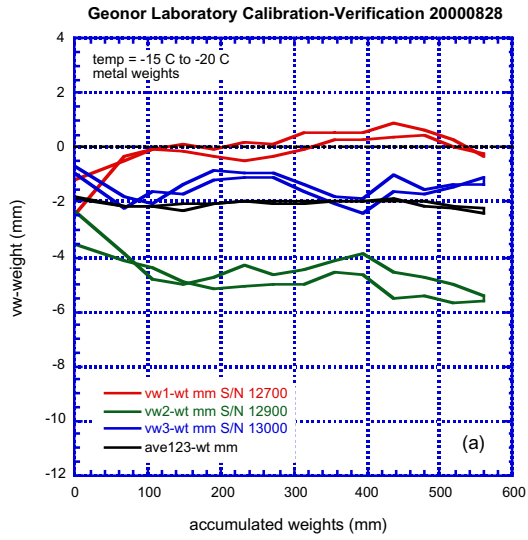


Fig. A.5

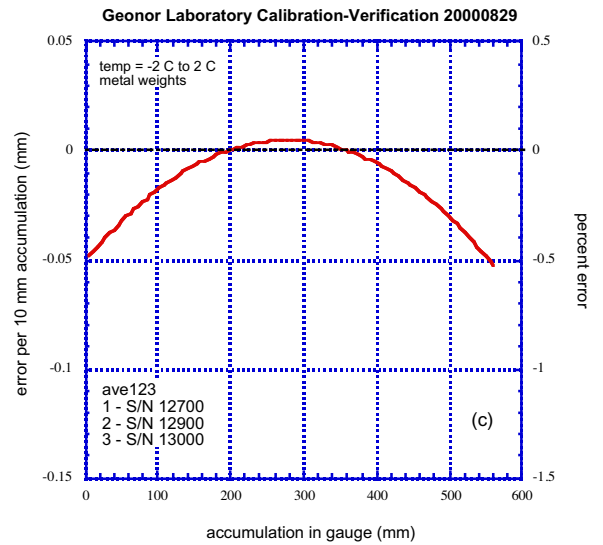
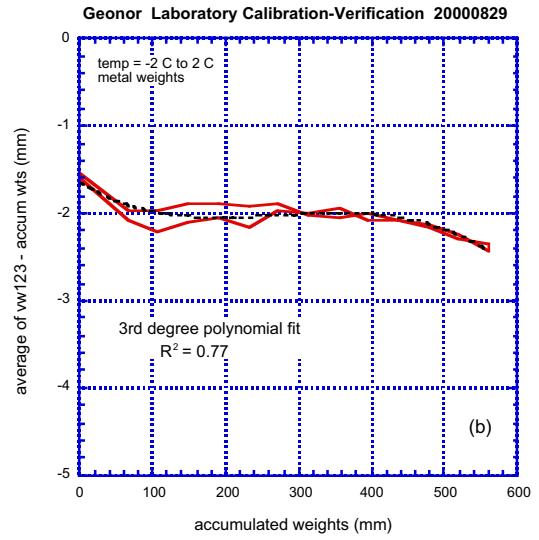
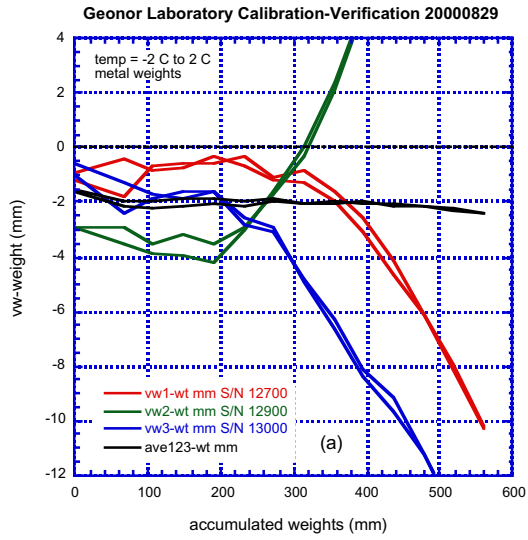


Fig. A.6

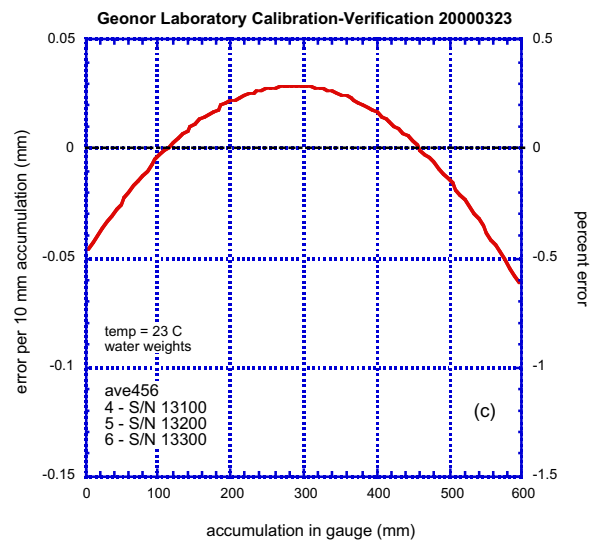
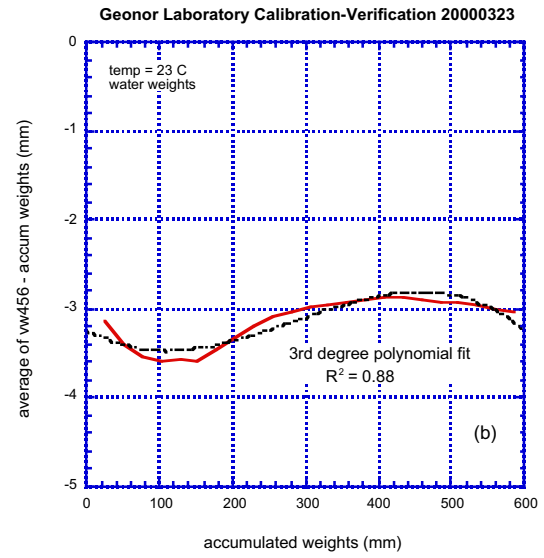
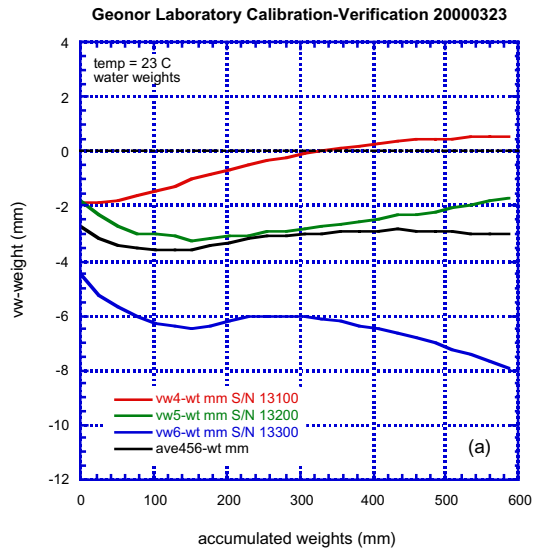


Fig. A.7

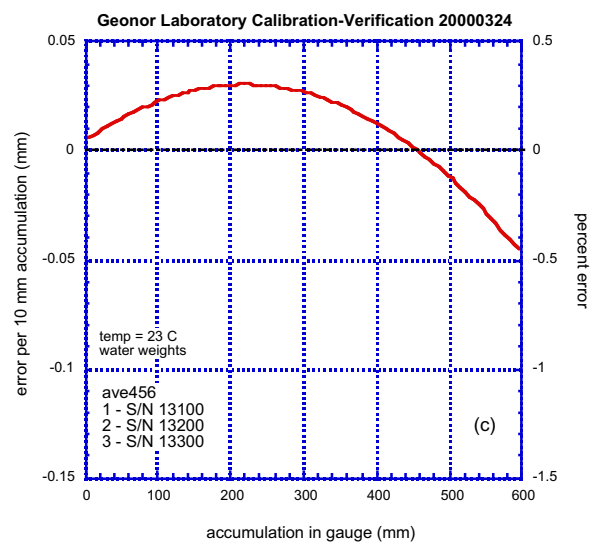
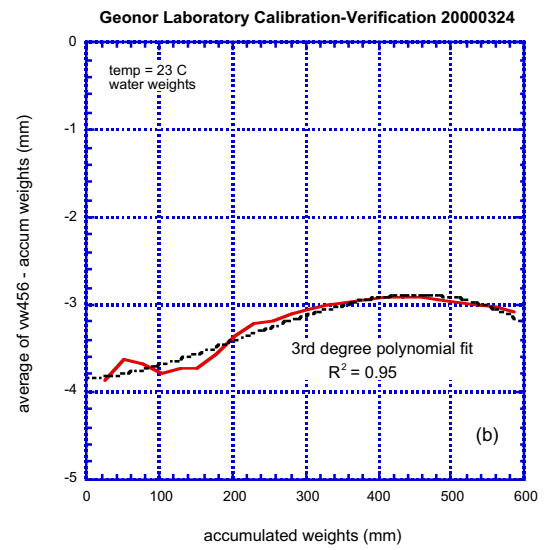
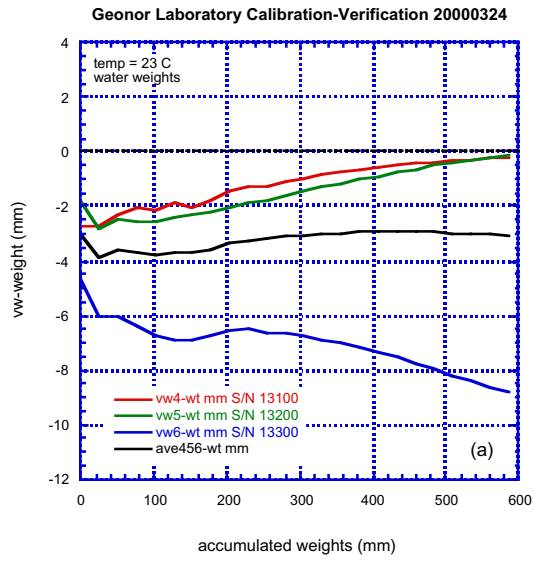


Fig. A.8

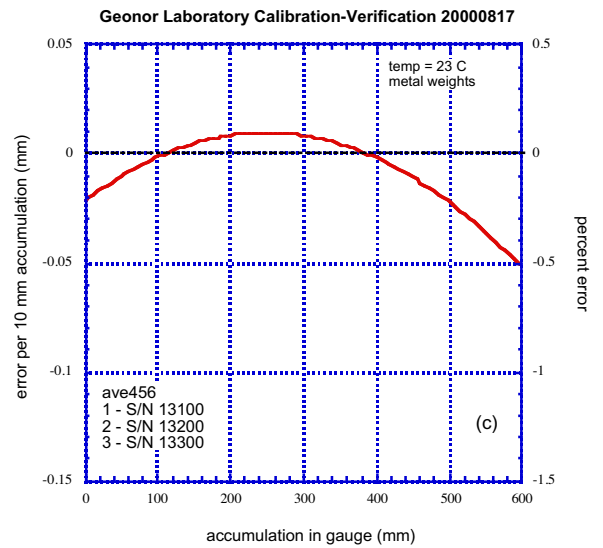
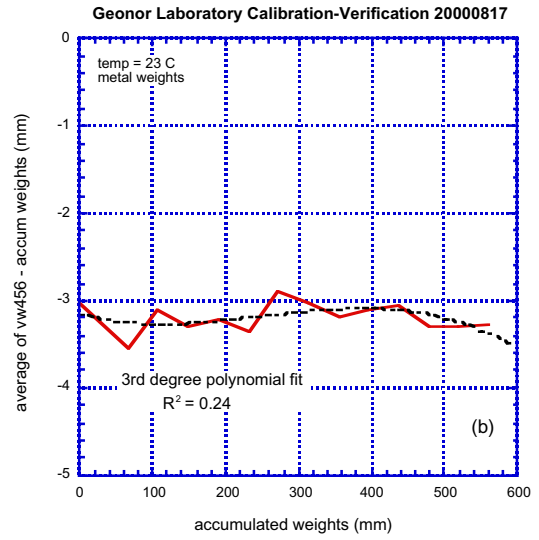
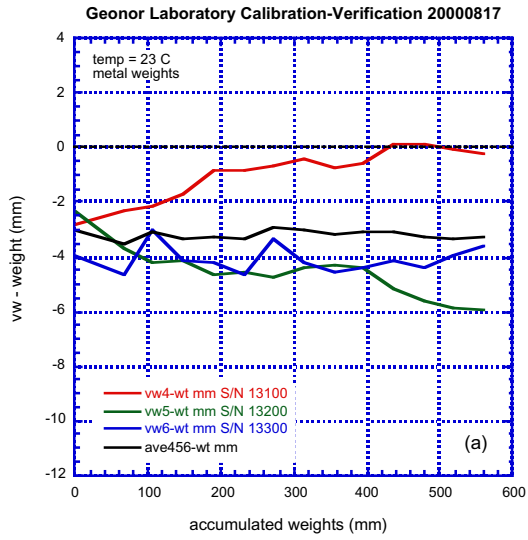


Fig. A.9

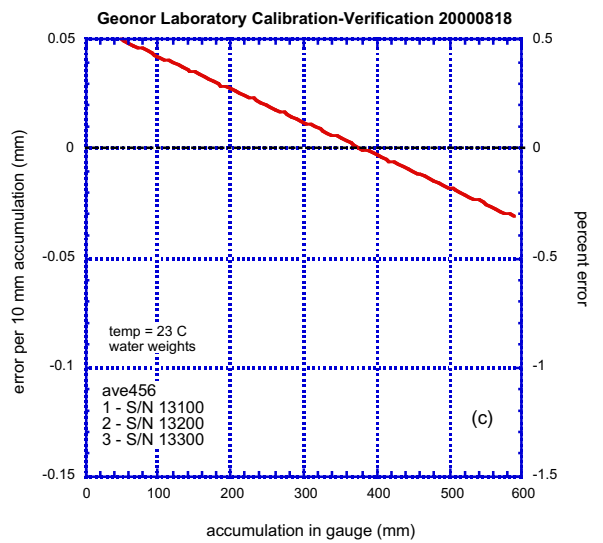
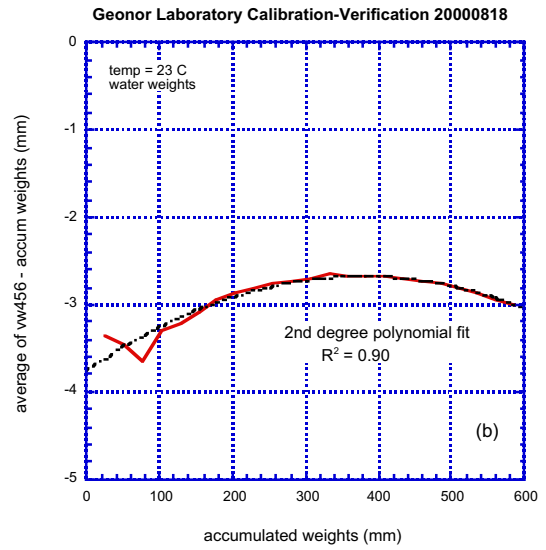
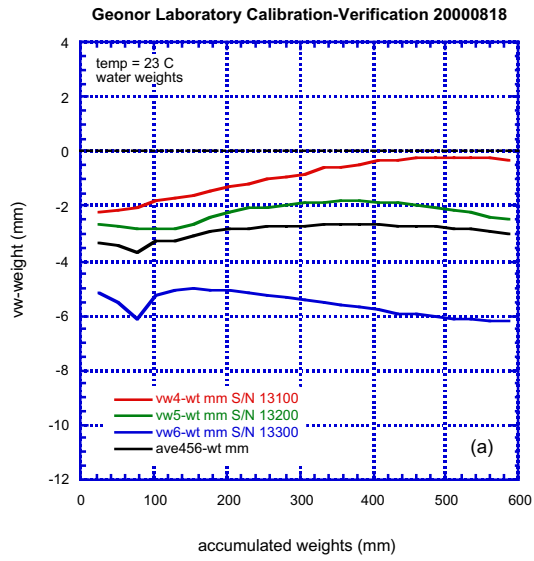


Fig. A.10

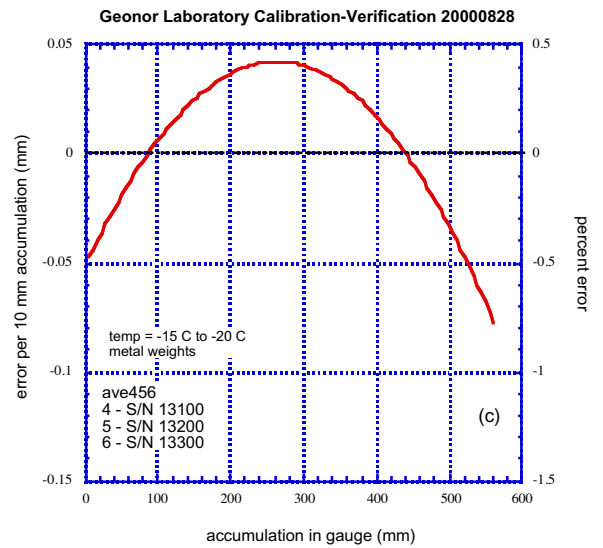
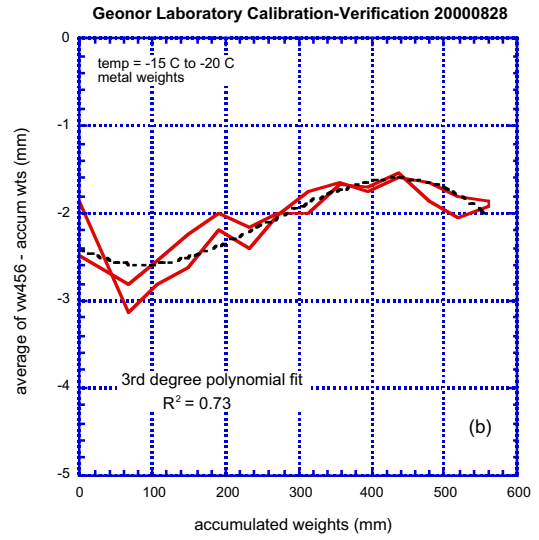
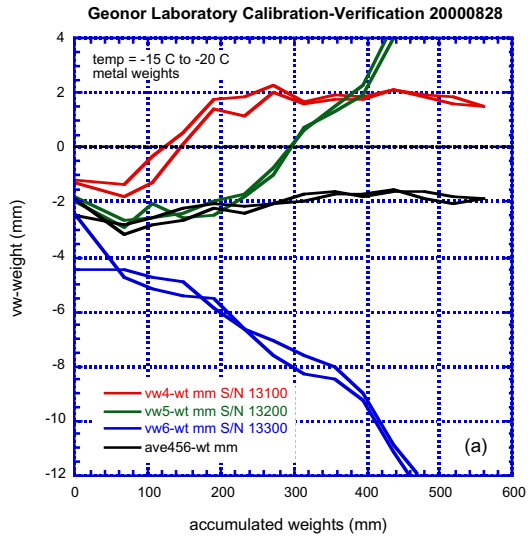


Fig. A.11

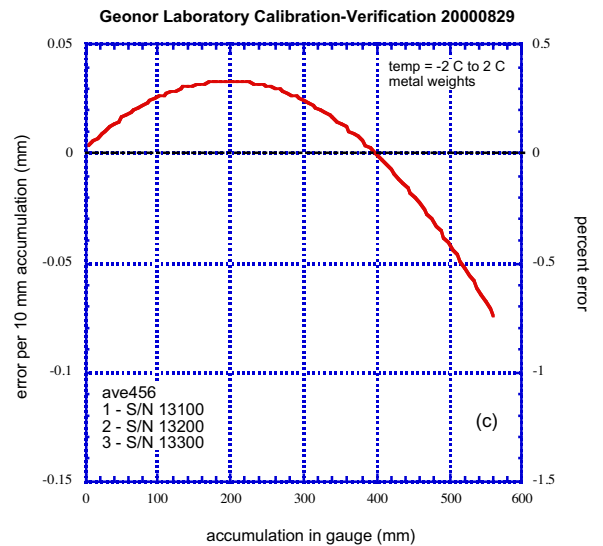
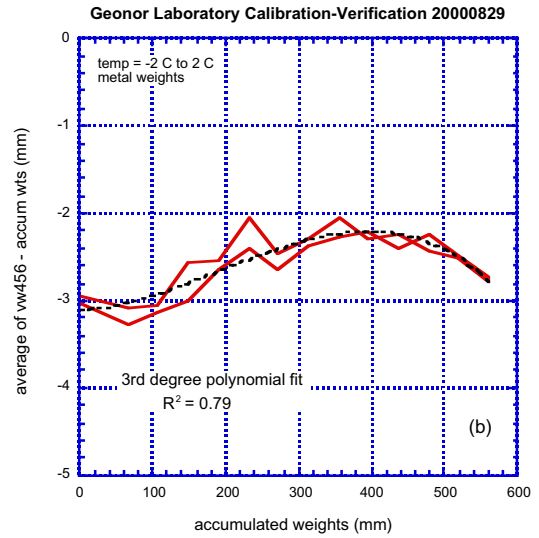
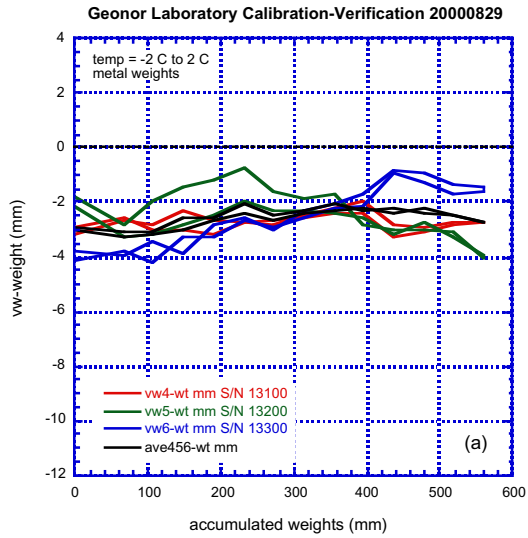


Fig. A.12

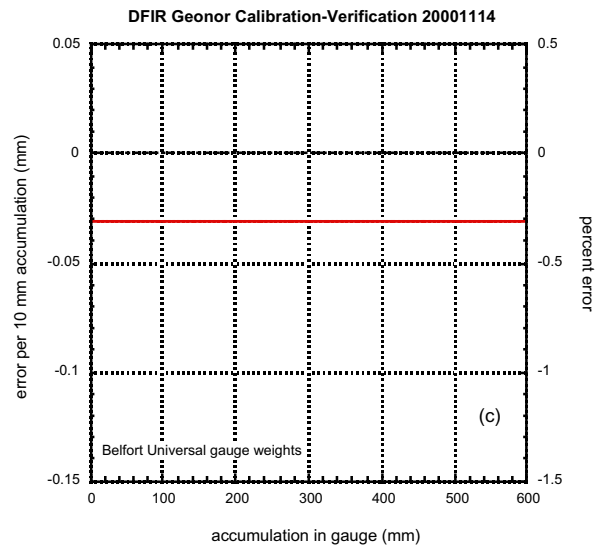
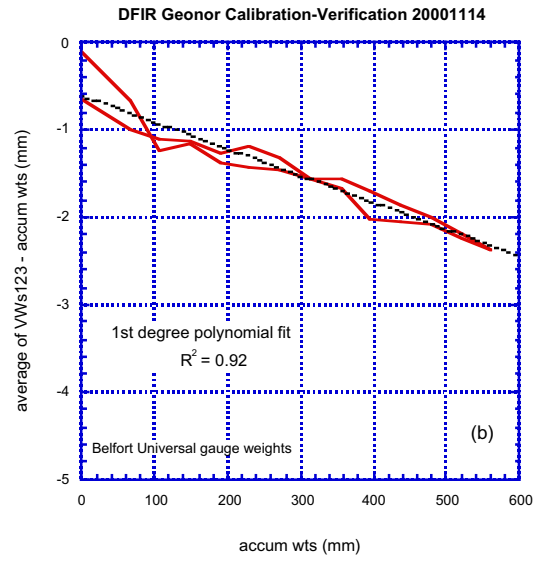
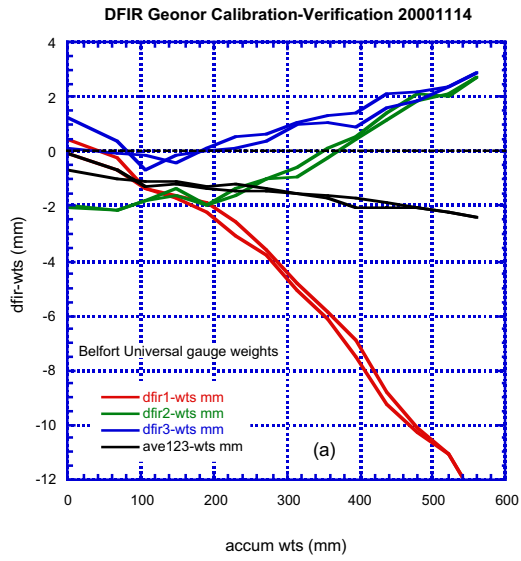


Fig. A.13

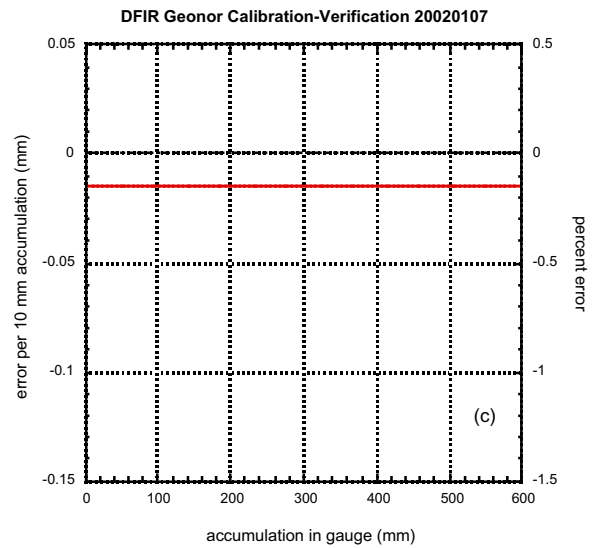
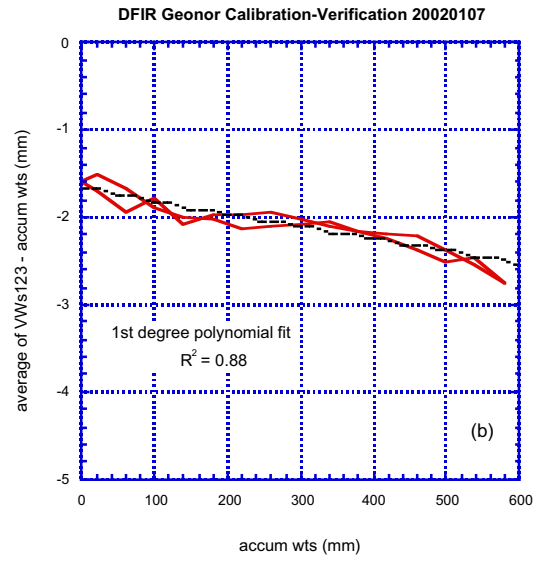
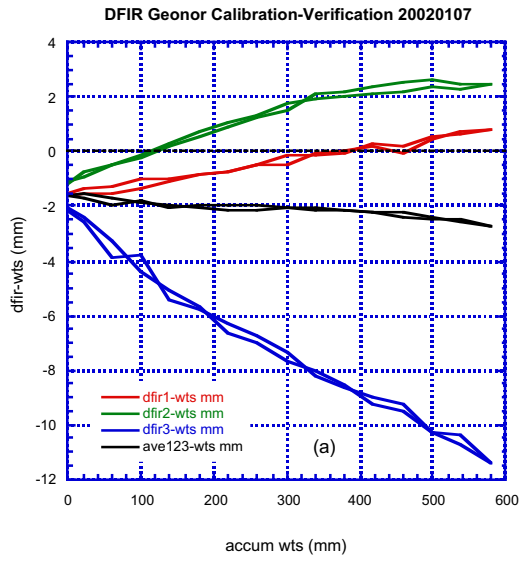


Fig. A.14

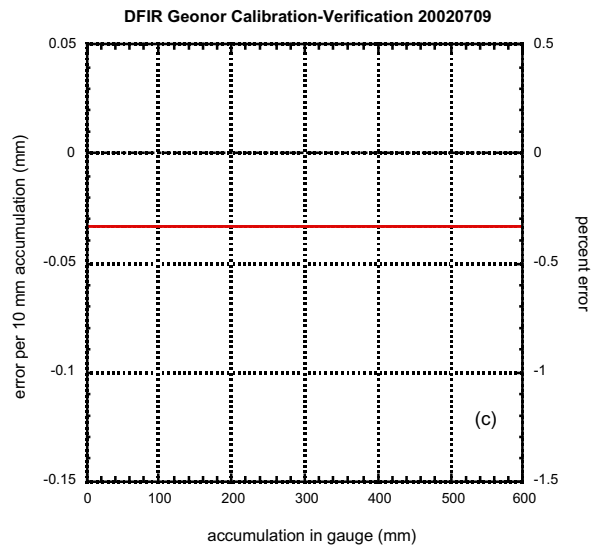
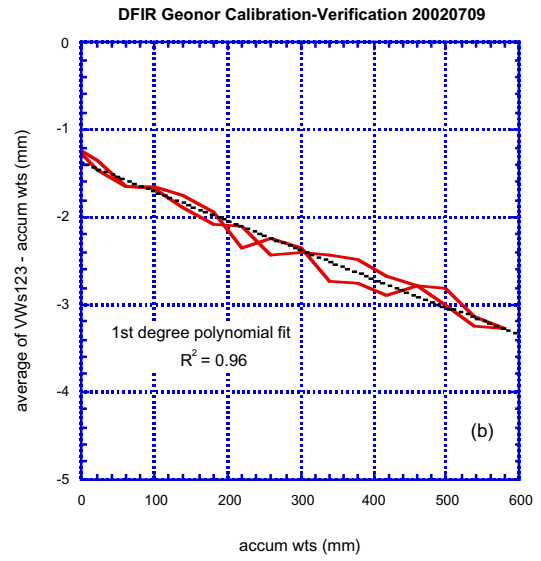
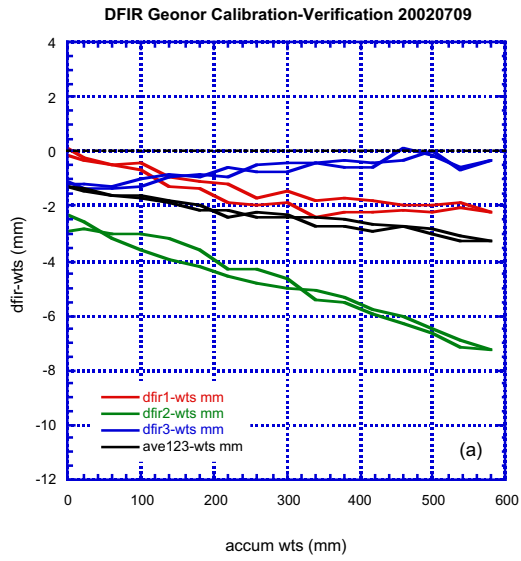


Fig. A.15

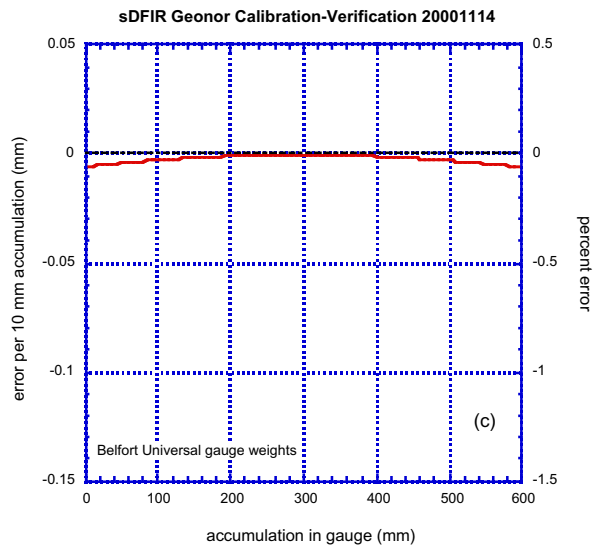
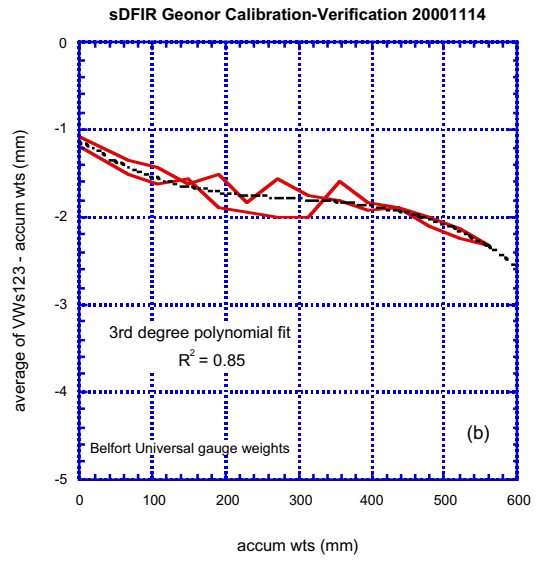
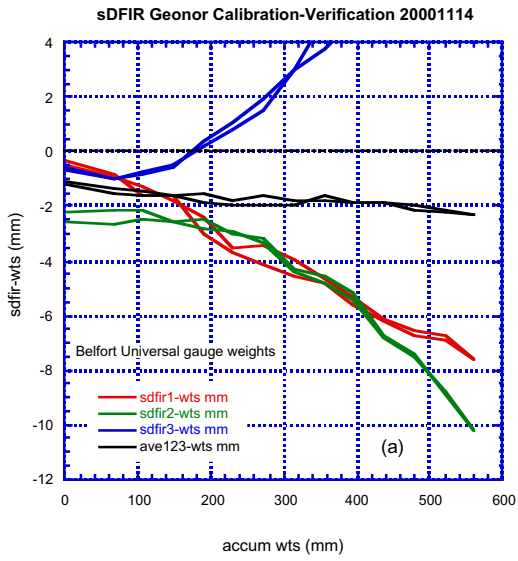


Fig. A.16

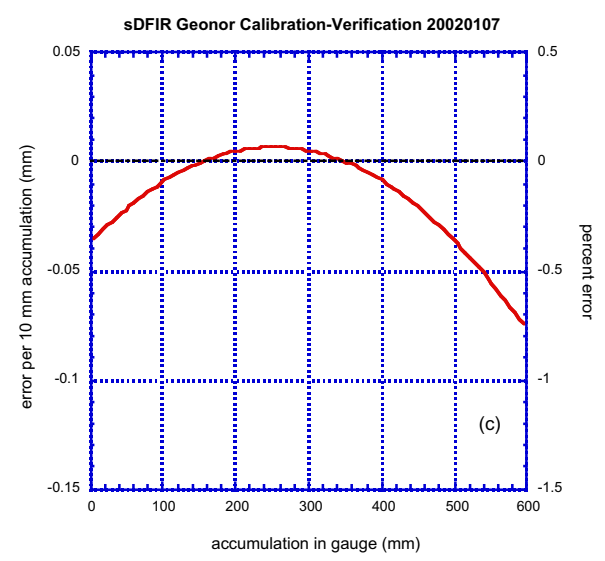
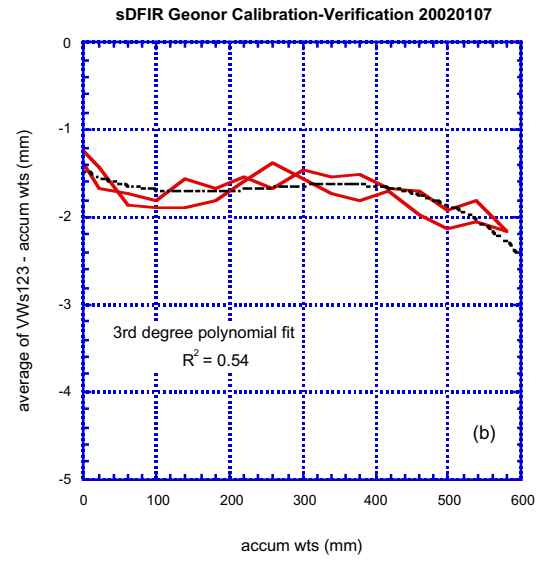
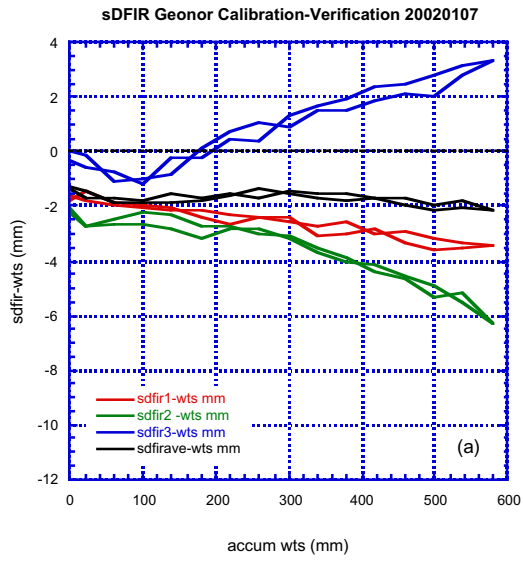


Fig. A.17

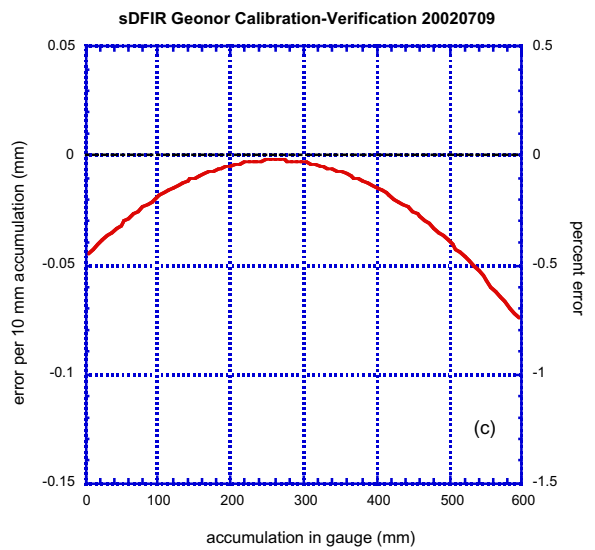
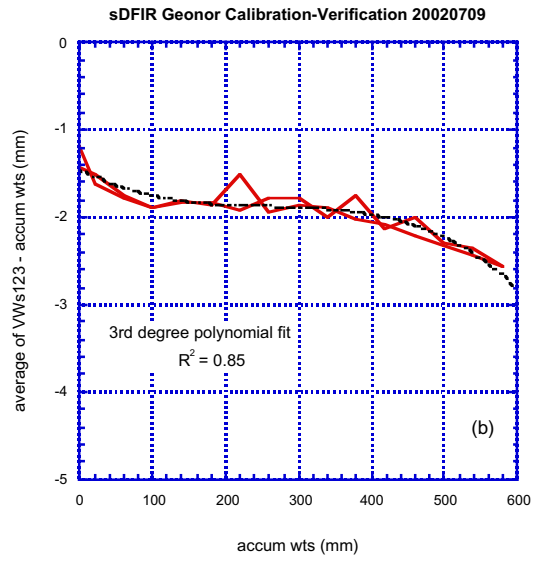
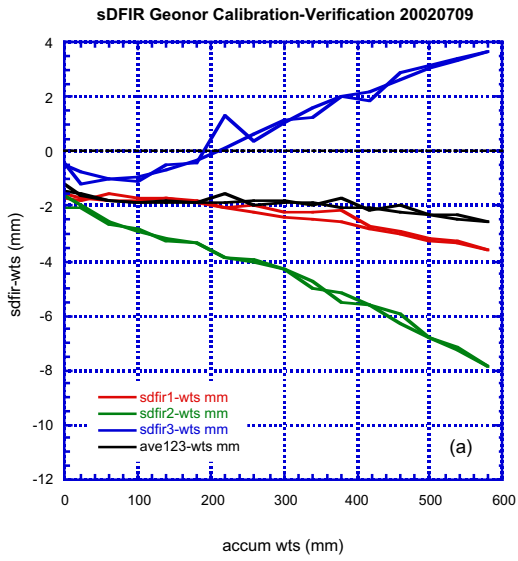


Fig. A.18

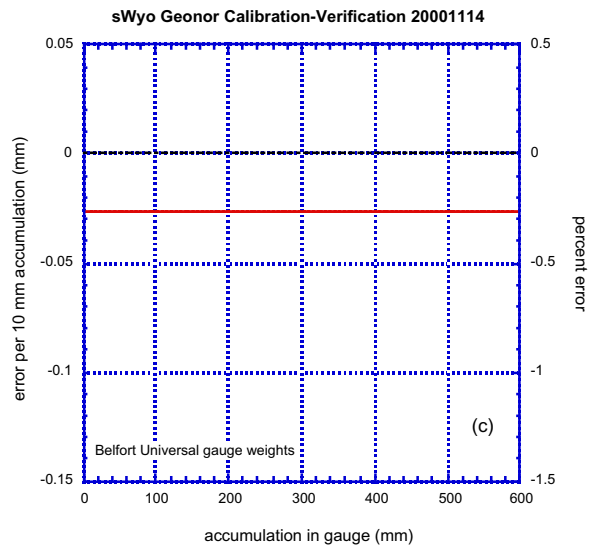
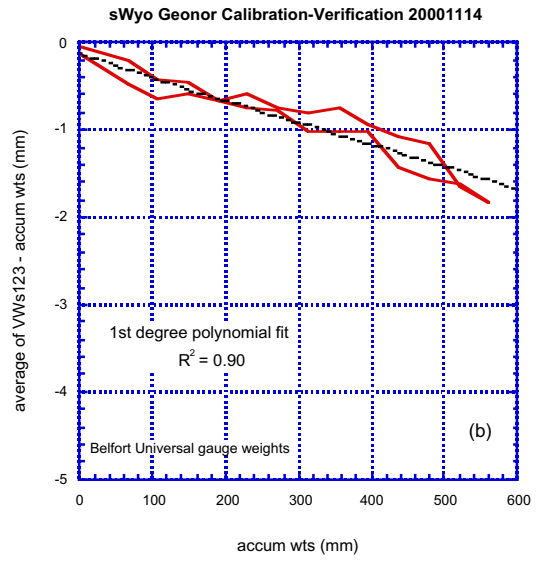
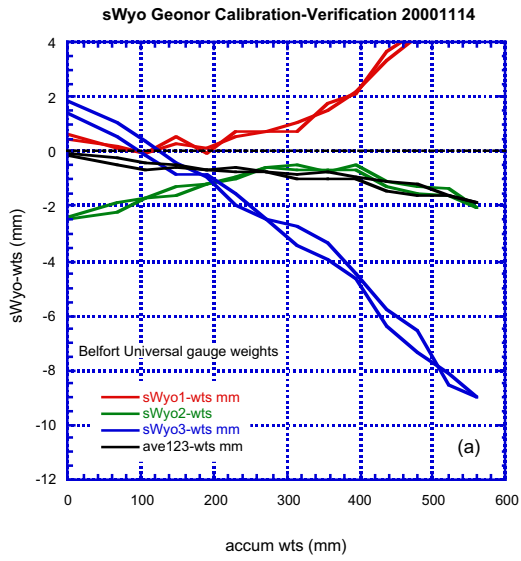


Fig. A.19

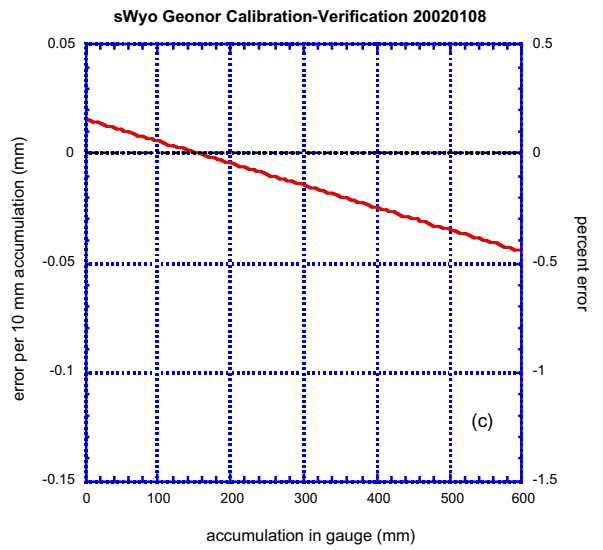
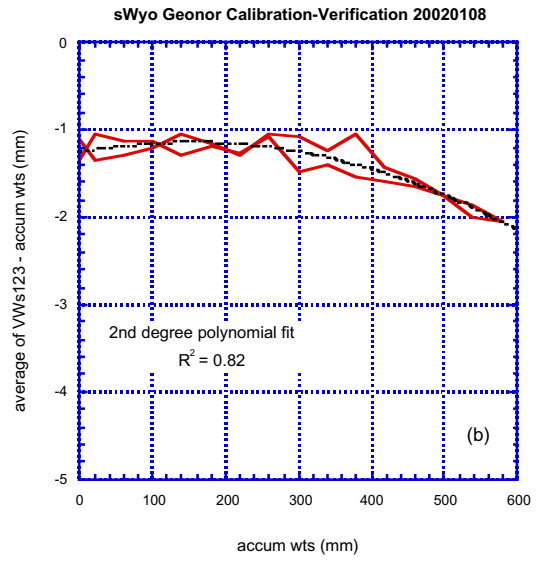
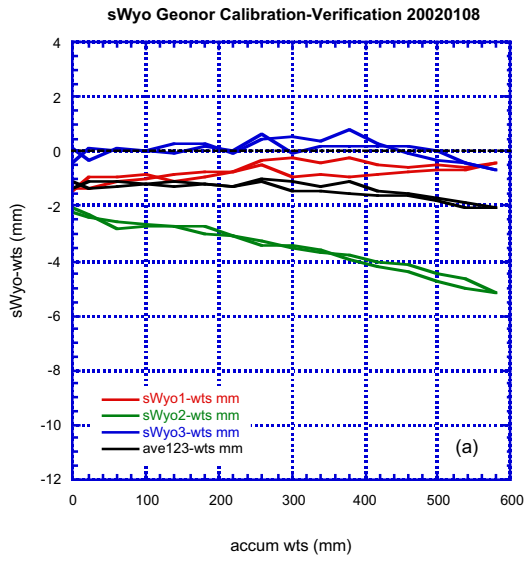


Fig. A.20

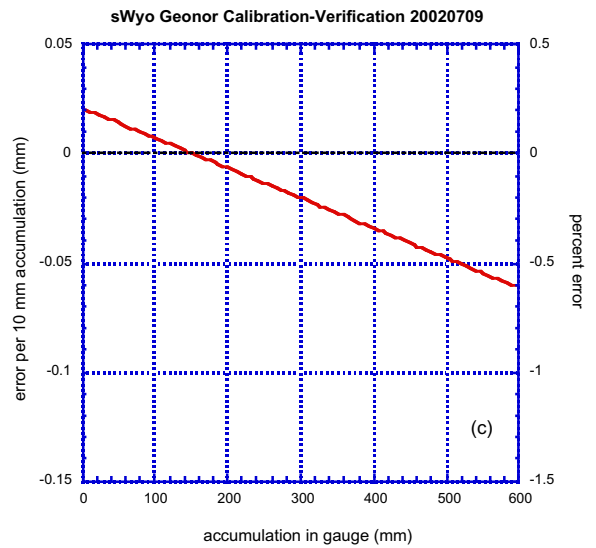
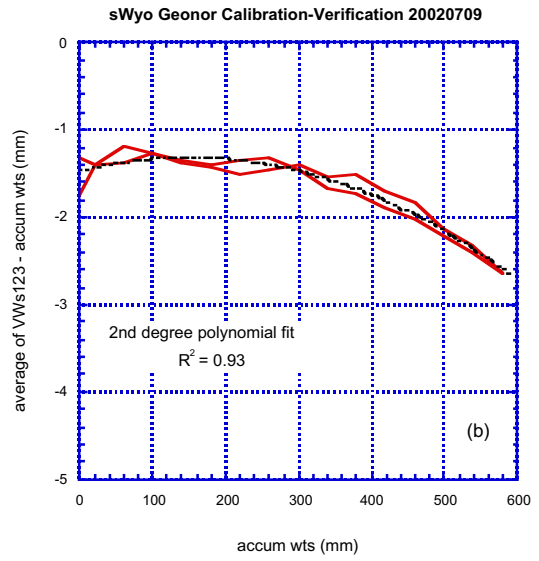
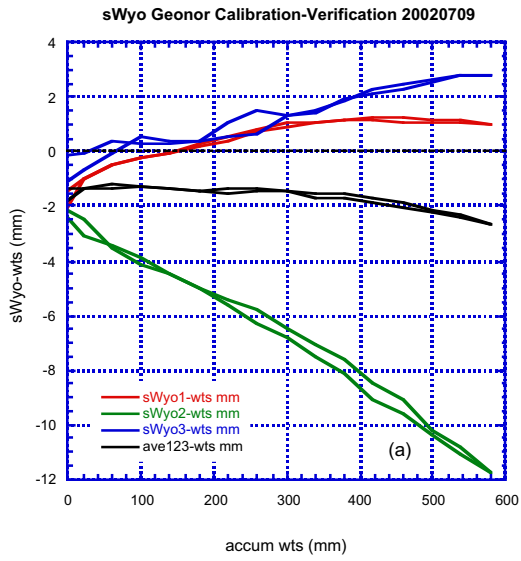


Fig. A.21

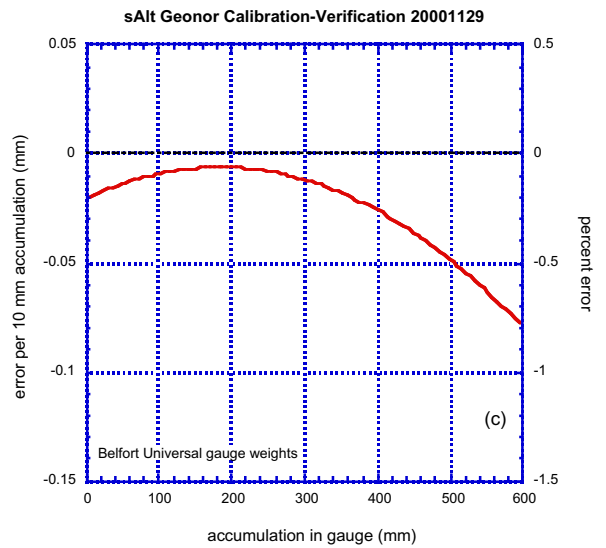
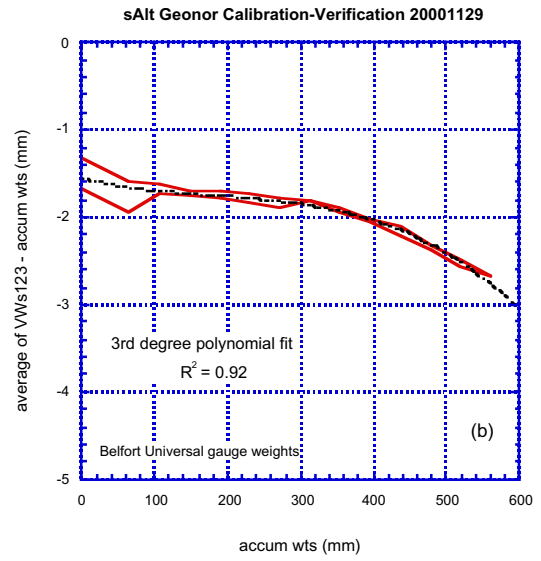
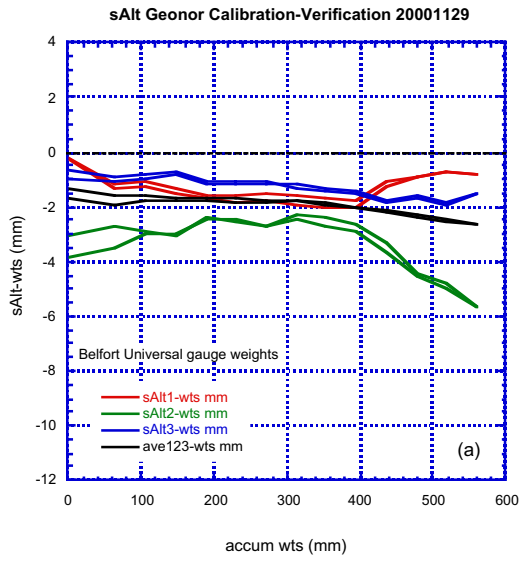


Fig. A.22

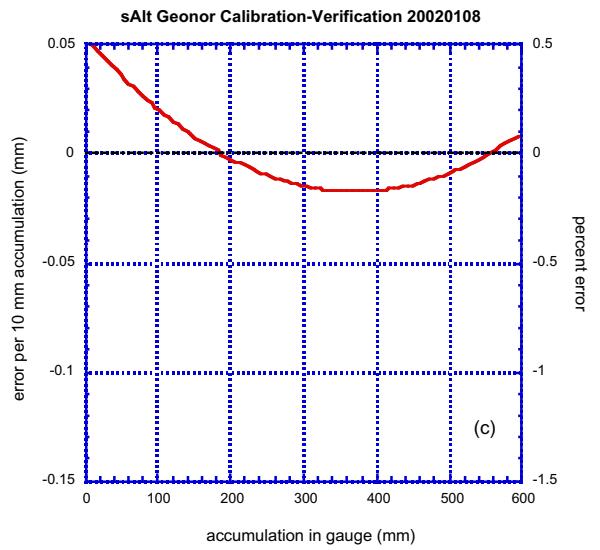
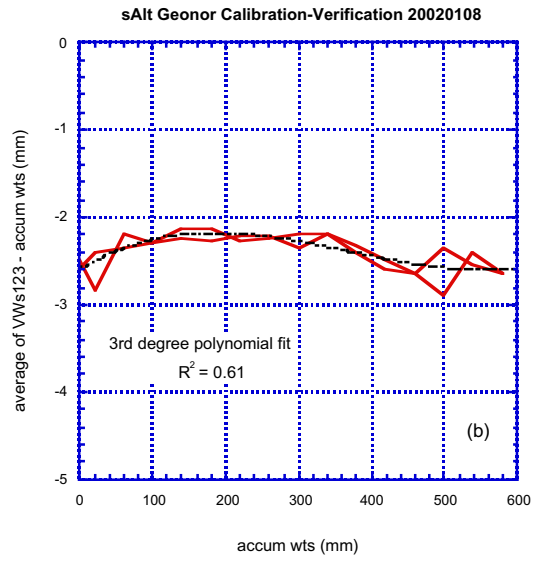
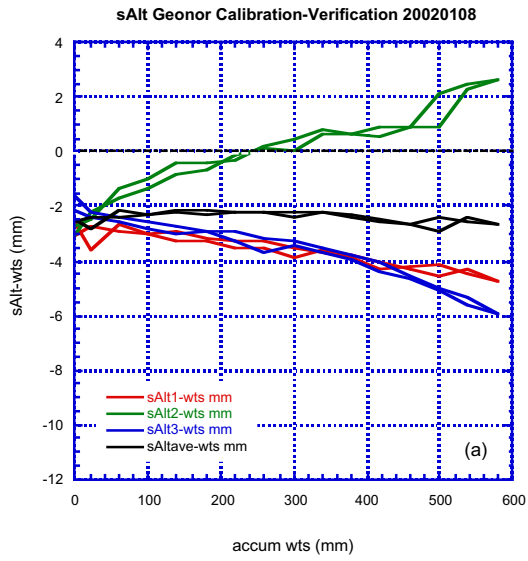


Fig. A.23

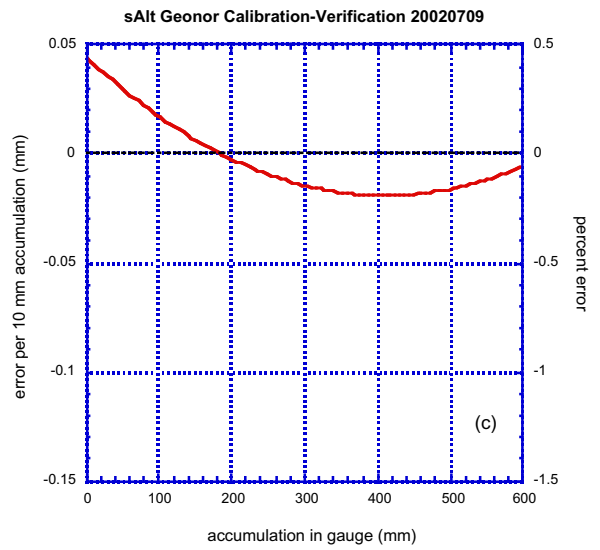
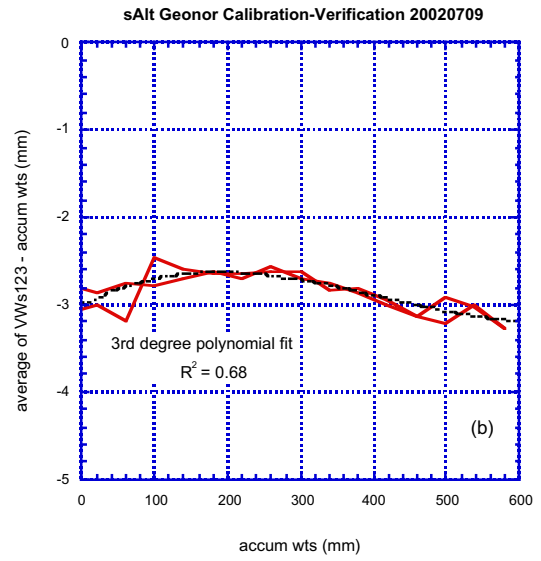
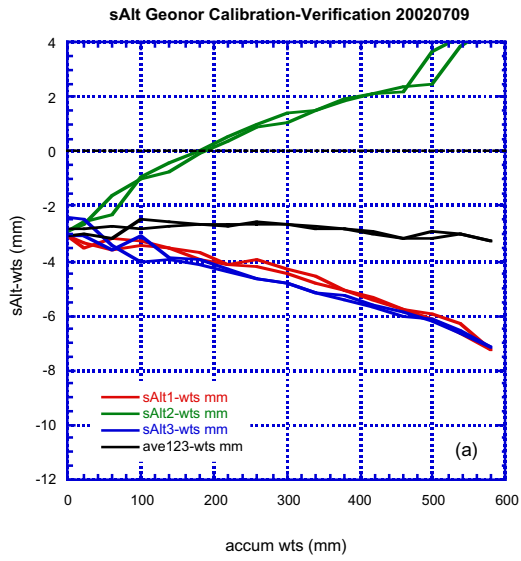


Fig. A.24

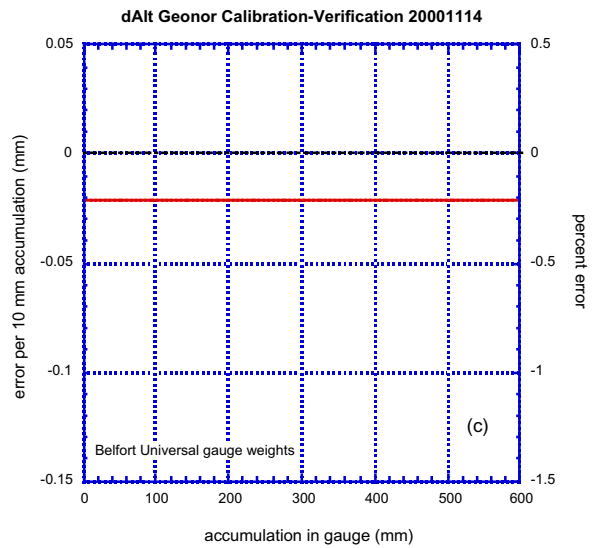
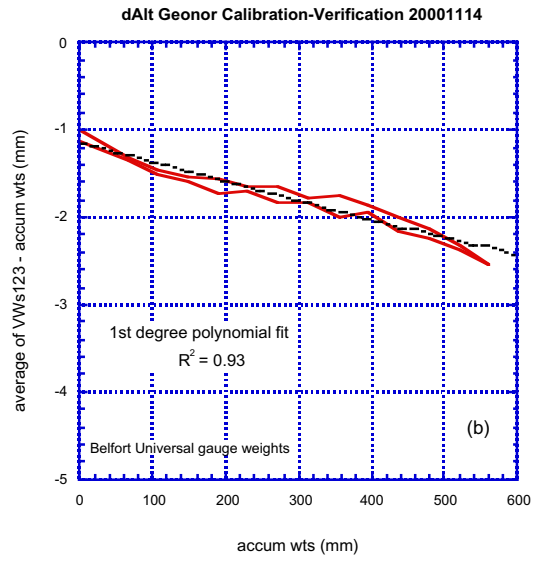
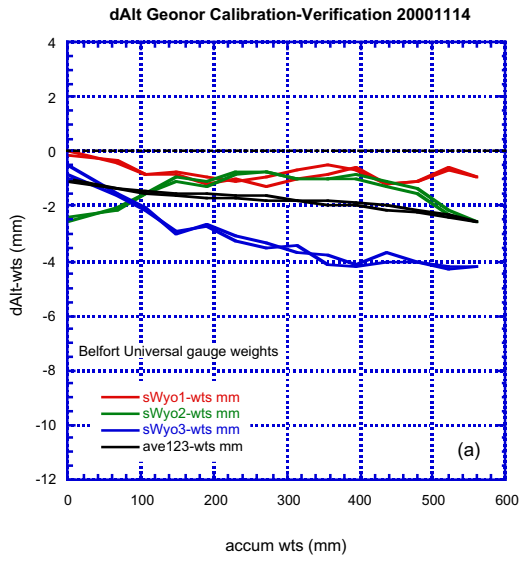


Fig. A.25

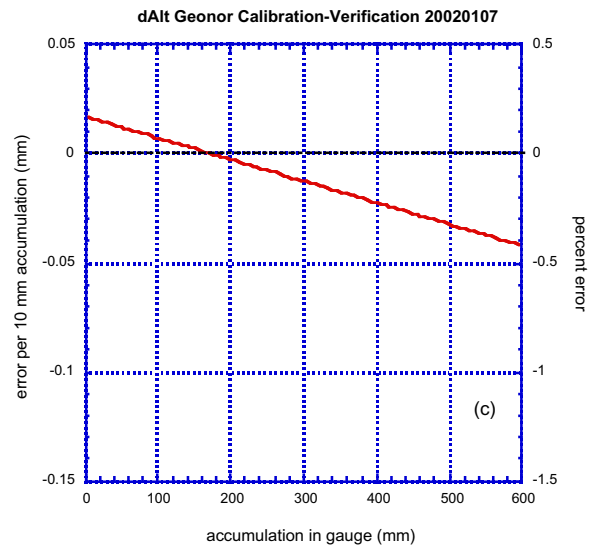
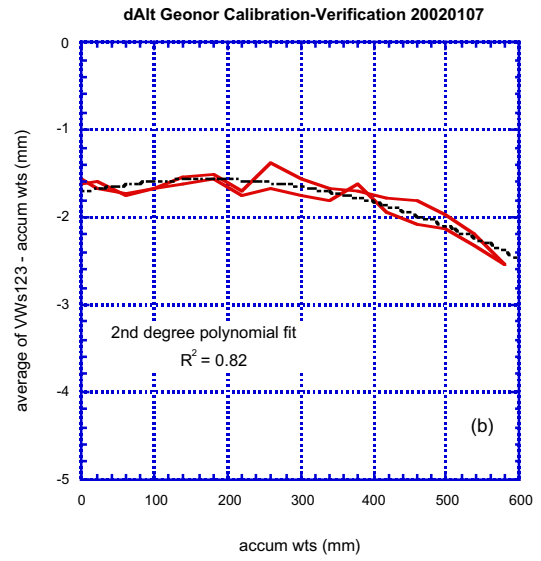
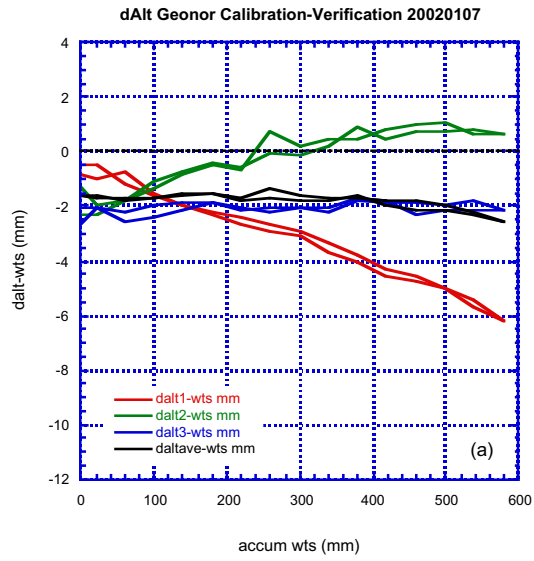


Fig. A.26

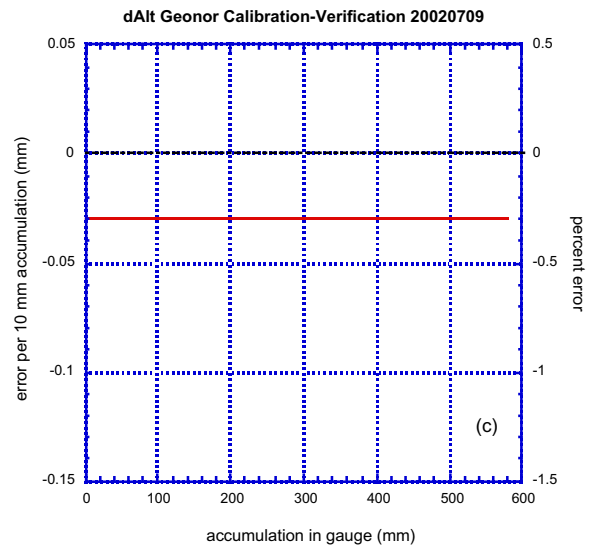
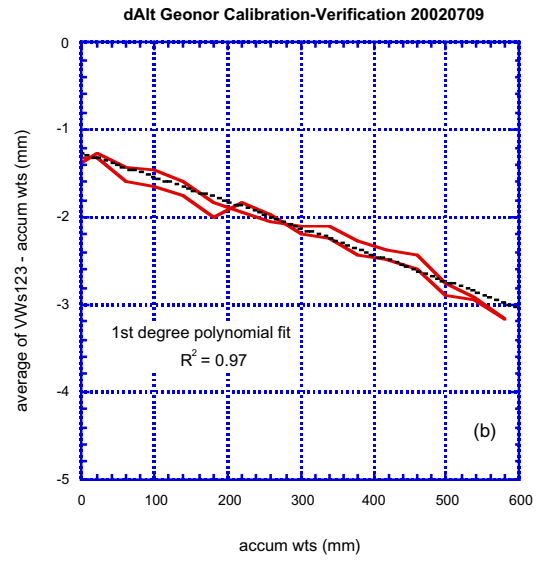
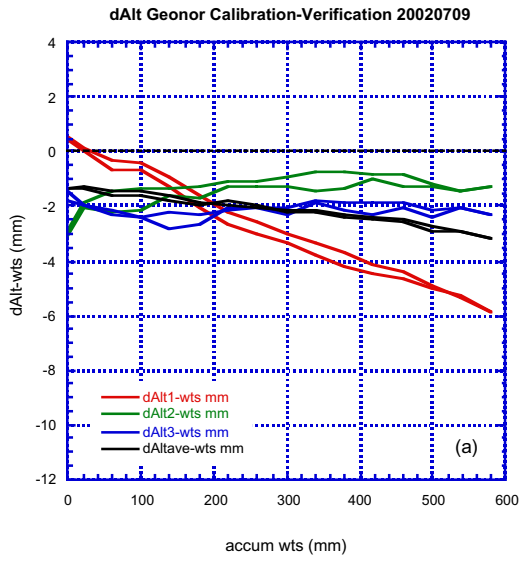


Fig.A.27

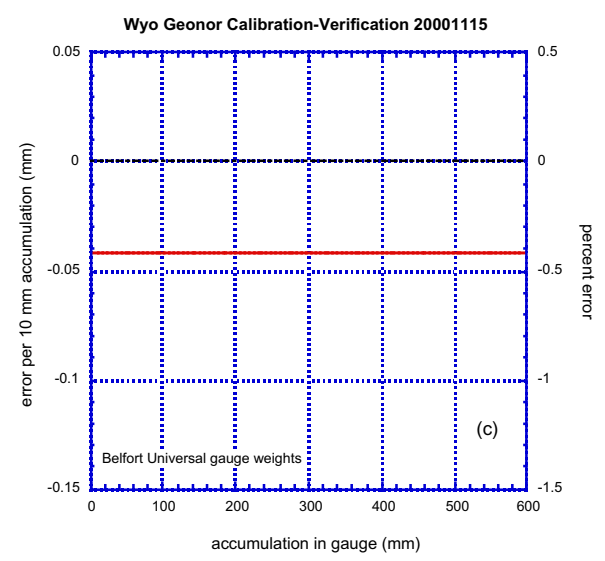
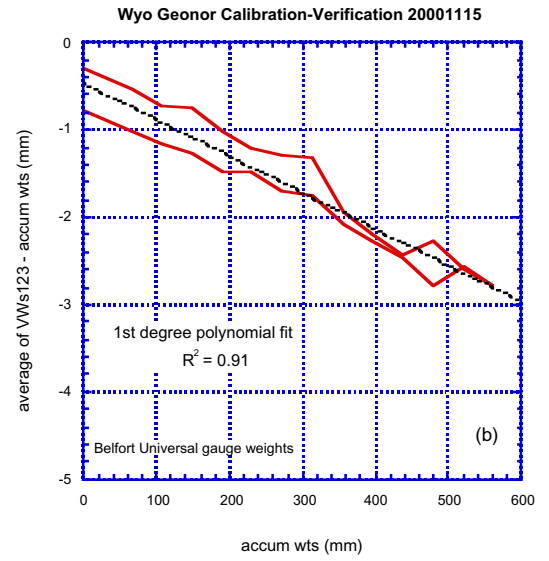
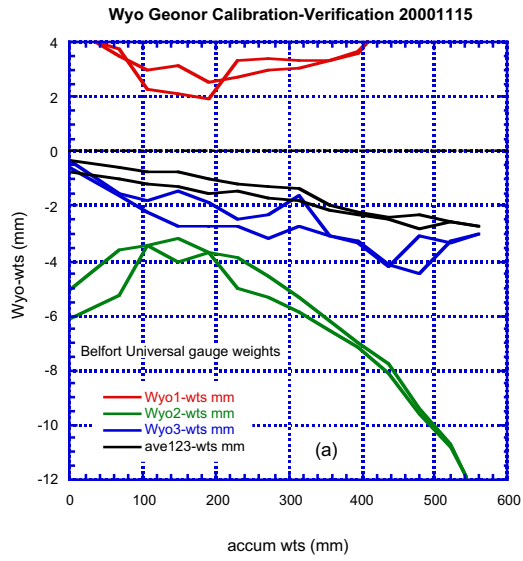


Fig. A.28

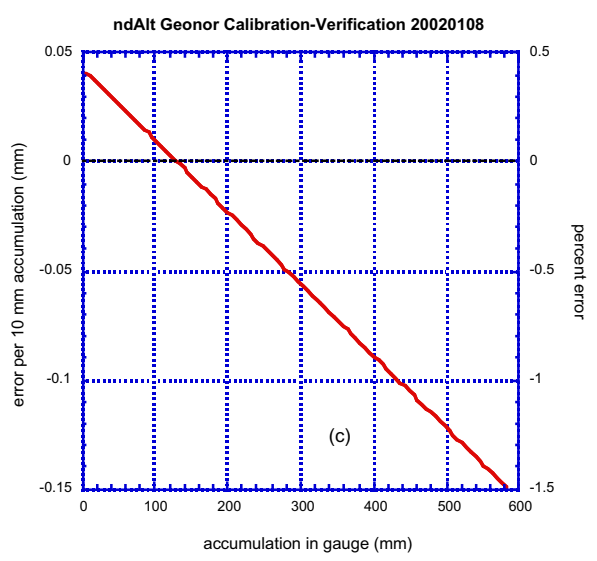
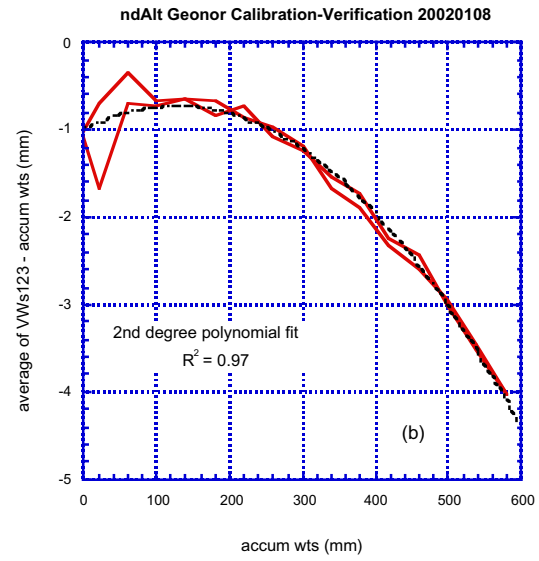
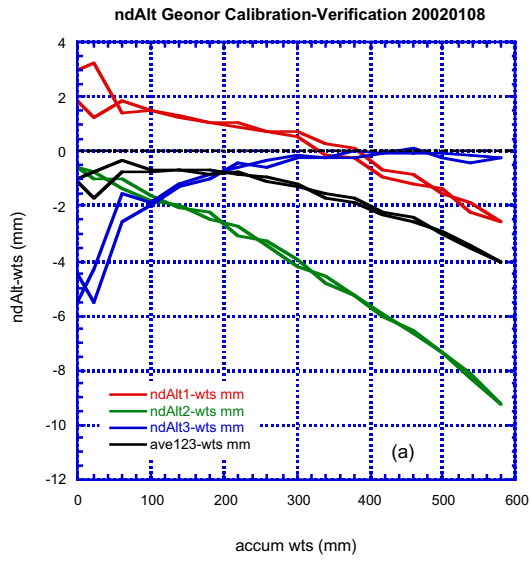


Fig. A.29

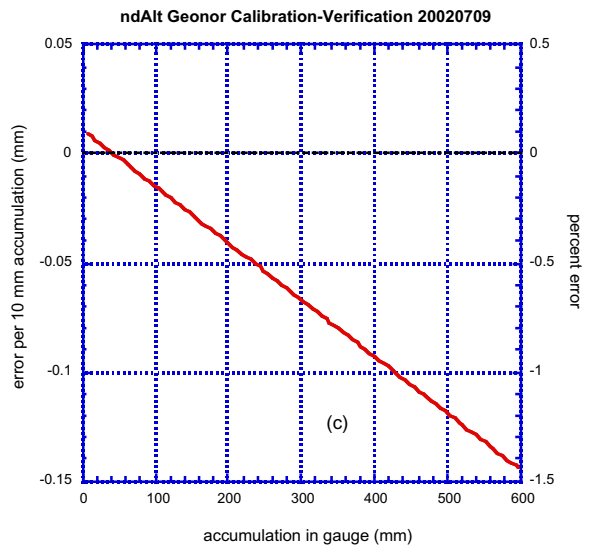
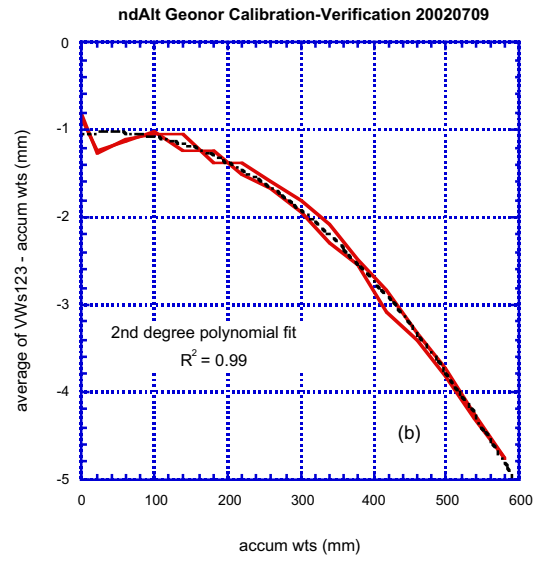
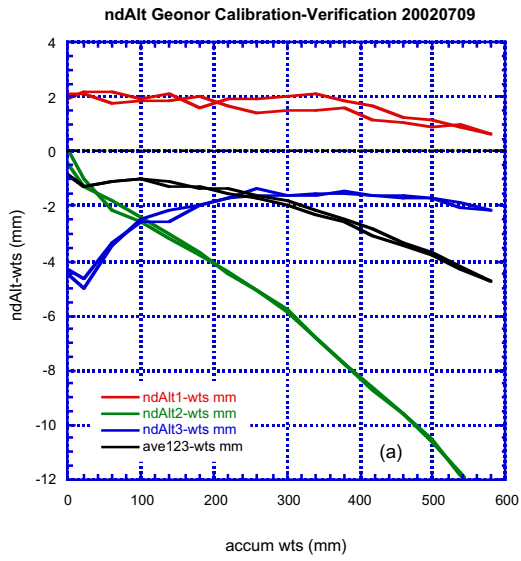


Fig. A.30